

CHAPTER IV

RESULTS AND DISCUSSION

1. Extraction and isolation of the ecteinascidins from the Thai tunicate, *Ecteinascidia thurstoni*

Et 743 is one of the marine natural products that possessed extremely potent cytotoxic activity and showed promising activity in phase II/III clinical trials. Therefore, a large amount of Et 743 is currently demanded for thoroughly investigations. To date, Et 743 has been supplied from both natural and synthetic sources. However, both available approaches are still low yield process. Thus, the KCN-pretreated strategy was applied to isolate the ecteinascidins-type compounds, which bear the labile α -carbinolamine functionality. In addition, the labile α -carbinolamine group was stabilized by converting to the more stable α -cyanoamine group. In 2002, Suwanborirux *et al.*, reported the isolation of Et 770 and Et 786 from the Thai tunicate using KCN-pretreated strategy. This strategy provides the advantage of increasing the yield of isolated natural ecteinascidins for further chemical and biological studies to develop this class of compound as new anticancer agents.

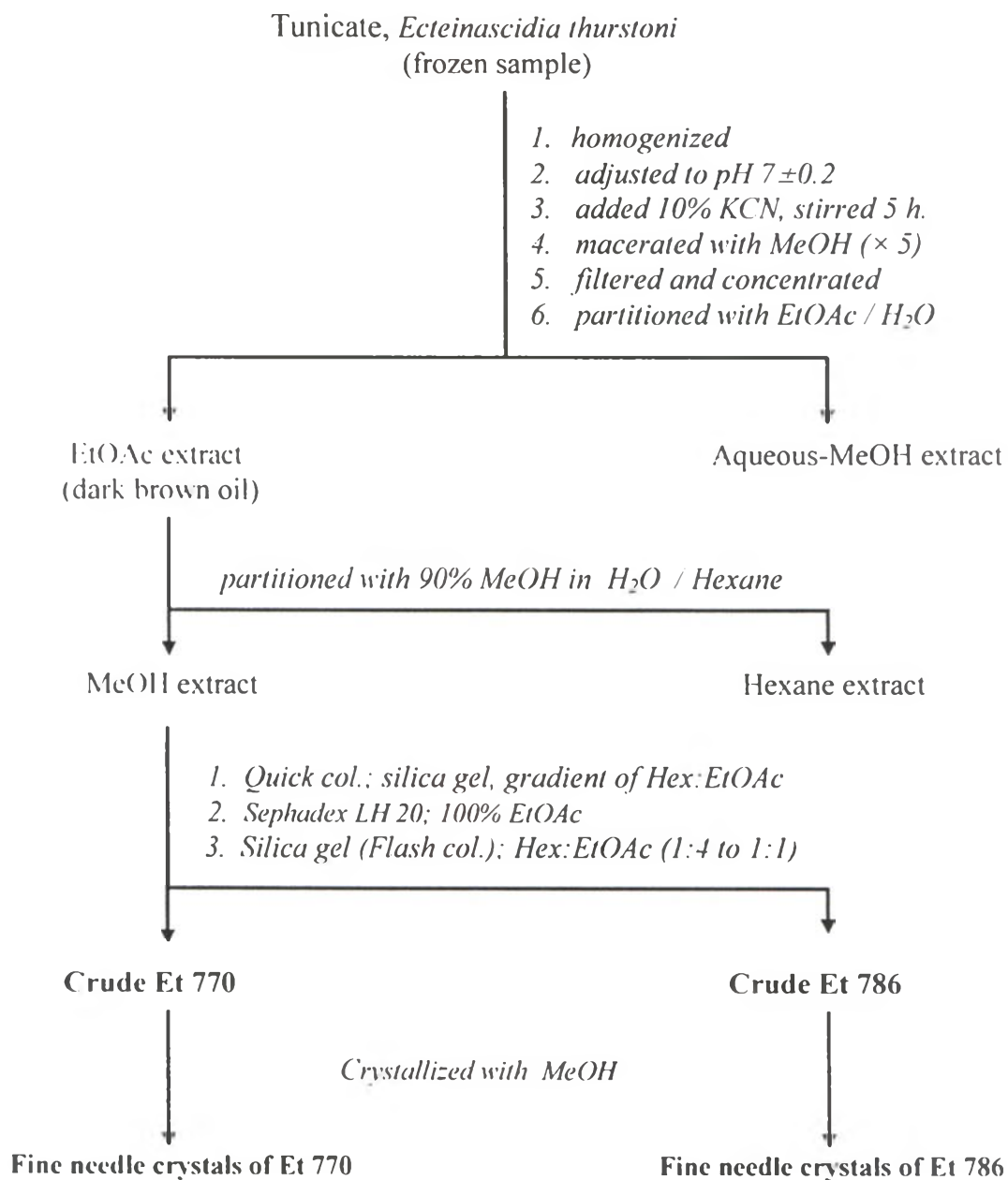
As the new biological source for ecteinascidin, the Thai tunicate *Ecteinascidia thurstoni* was collected from Phuket Island in the southern part of Thailand. The identification and characterization of the Thai tunicate were conducted, mainly on the basis of its morphological characteristics. However, the biodiversity information of the Thai tunicate is unclear, therefore our collection has been conducted following the blooming period of the Thai tunicate. For this research, four collections of tunicate were done in October 2002 (No. 1), January 2003 (No. 2), June 2003 (No. 3) and July 2003 (No. 4), which were stored frozen until use. Herein, the four collected tunicate samples were subjected to two separated isolation procedures as shown in Scheme 18 and the data of each isolation results were showed in Table 11.

The homogenized sample of the combined collections No. 1 and 2 (total 64.4 kg of weight wet) was pretreated with potassium cyanide and macerated with methanol to afford an aqueous emulsion, upon filtration and concentration. It was further extracted with ethyl acetate and subjected to partition between hexane and 90% methanol in water to give the methanolic extract, which was continuously fractionated with silica gel quick column chromatography, Sephadex LH-20 gel filtration and silica gel flash column chromatography respectively, to give crude products of Et 770 (1.40 g) and Et 786 (0.44 g). Then the crude products were crystallized with methanol to afford the fine needle crystals of Et 770 (935.5 mg, 1.5×10^{-3} % yield of wet wt.) and Et 786 (243.0 mg, 3.8×10^{-4} % yield of wet wt.), whereas the isolated ecteinascidins from the Caribbean tunicate *Ecteinascidia turbinata* were isolated in a lower yields (1.0×10^{-4} % to 1.0×10^{-5} % yield of wet animal) (Rinehart *et al.*, 1990). Both isolated compounds were structurally elucidated by comparison with the authentic sample (Suwanborirux *et al.*, 2002), which were identical in all respects.

The recollection tunicates batches No. 3 and No. 4 were conducted in a similar procedure to the first collection as described in Scheme 18 to give the natural ecteinascidins which was summarized in Table 11. The total isolated Et 770 (1.4 g) and 786 (435.5 mg) were used as the synthetic starting materials for this study.

Table 11. Isolation data of Et 770 and Et 786 of each tunicate collection

No collection	Collection period	Animal weight (kg, wet wt.)	EtOAc ext. (g)	Et 770		Et 786	
				Weight (mg)	% yield of wet wt.	Weight (mg)	% yield of wet wt.
1	October 2002	47.9	53.3	935.5	1.5×10^{-3}	243.0	3.8×10^{-4}
2	January 2003	16.5					
		64.4					
3	June 2003	60.0	72.3	490.3	6.8×10^{-4}	192.5	2.7×10^{-4}
4	July 2003	12.0					
		72.0					
Total		136.4 kg	125.6 g	1.4 g	1.1×10^{-3}	435.5 mg	3.0×10^{-4}

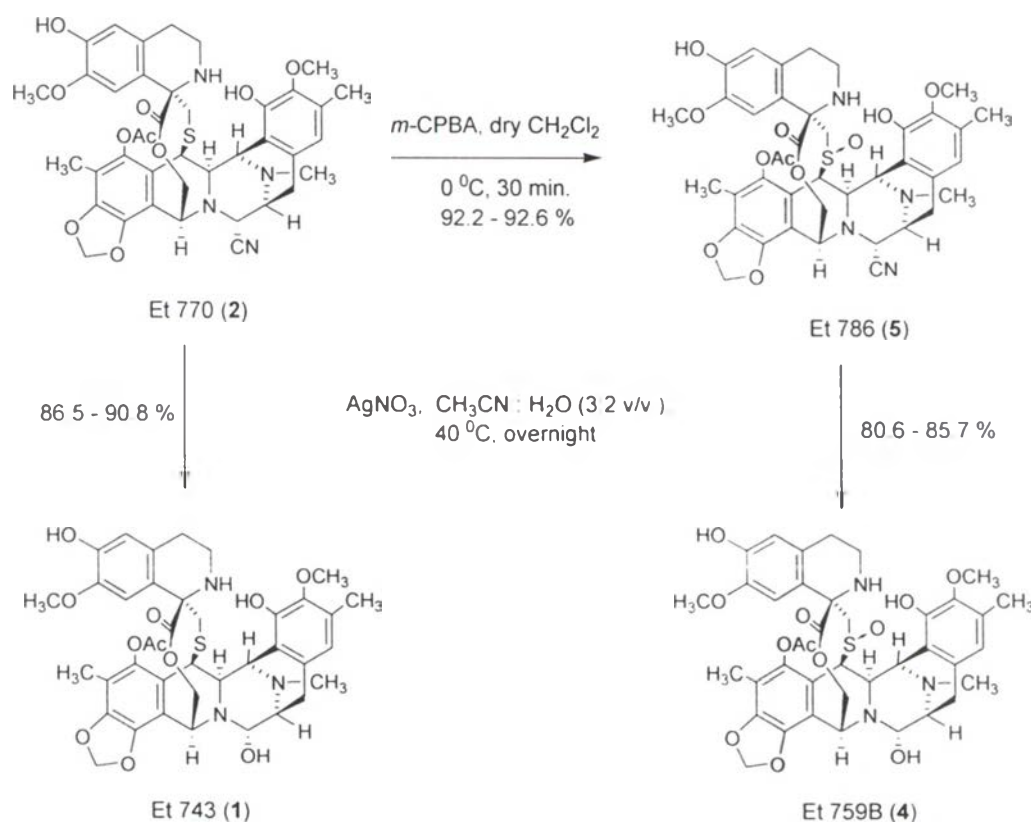


Scheme 18. The extraction and isolation methods of Et 770 and Et 786 from *Ecteinascidia thurstoni*

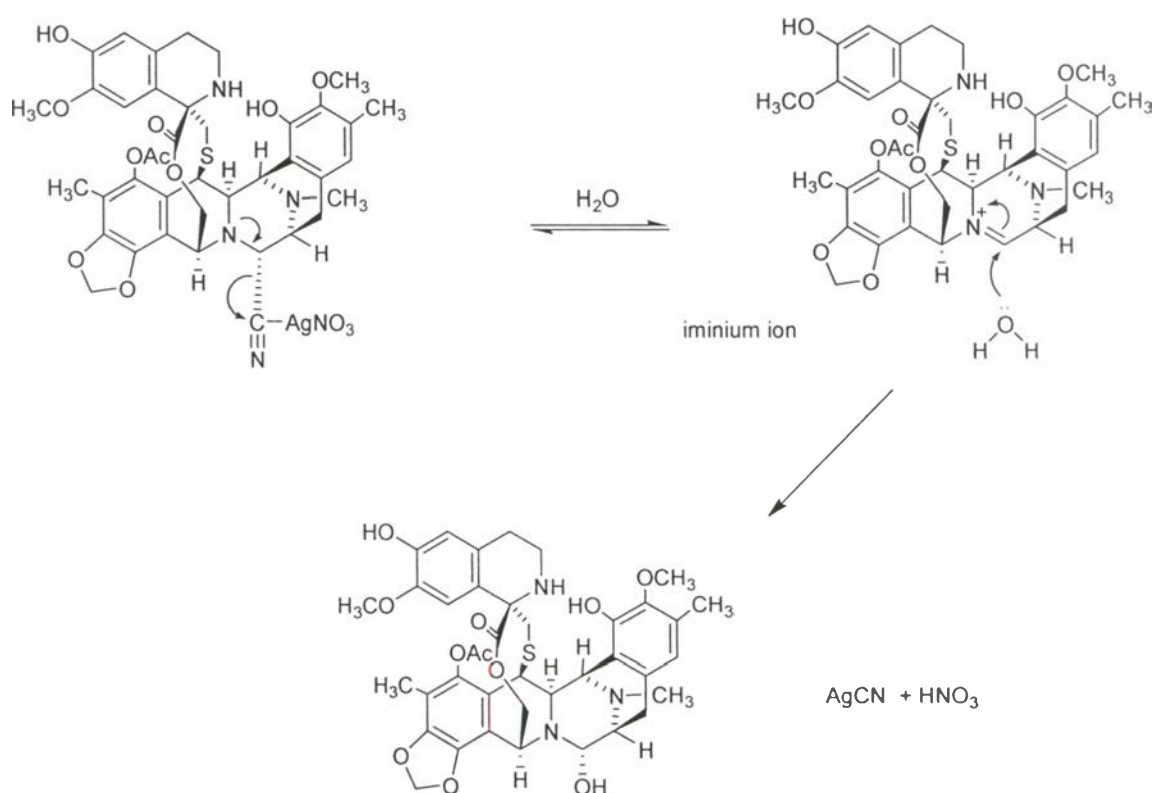
2. Structural modification

2.1 Transformations of Et 770 to Et 743 and Et 786 to Et 759B

Our first attempt is to convert the stable α -cyanoamine-containing Et 770 and Et 786 to their α -hydroxyamine parents compound as Et 743 and Et 759B, respectively. The initial step, the α -cyano group on the stable ecteinascidin (Et 770) was transformed to α -hydroxyl group in the presence of 25 equivalent amount of silver nitrate in the mixture solution of acetonitrile:water (3:2 v/v) at 40 °C to afford the product (Et 743) in the range of 86.5-90.8% yield and also Et 786 was converted to Et 759B in the range of 80.6-85.7% yield (Scheme 19). In this reaction, silver nitrate was used to catalyze the generation of an iminium intermediate type, which was allowed to react with a nucleophile. The reaction could be explained by assuming a S_N1 mechanism *via* an iminium ion intermediate as illustrated in Scheme 20.

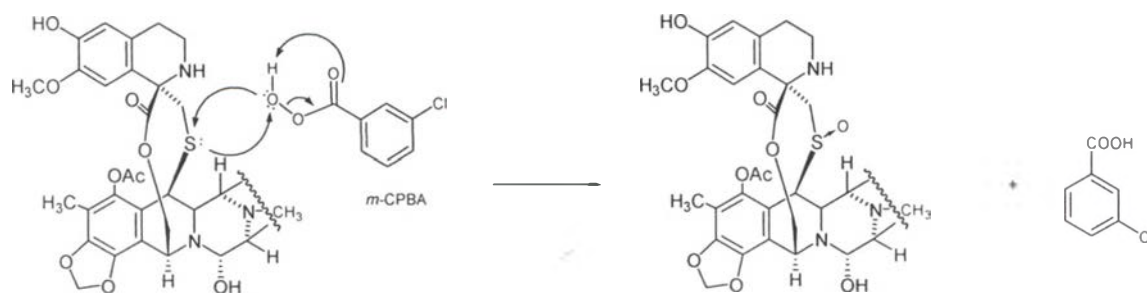


Scheme 19. Transformation routes of Et 770 to Et 743, and Et 786 to Et 759B



Scheme 20. The proposed mechanism of hydroxylation reaction *via* an iminium ion intermediate

The oxidation of sulfide to the corresponding sulfoxide can be achieved by a wide range of oxidizing agents, including various peroxy carboxylic acids. Thus, the sulfide on ecteinascidin molecule, Et 770, is oxidized under mild condition by 1.1 equiv of *m*-chloroperbenzoic acid (*m*-CPBA) at 0°C to obtain sulfoxide in high yield (92 %) and the product is free from the sulfone derivative. The proposed mechanism of reaction is depicted in Scheme 21. The chemical structure of those synthetic compounds were analyzed by NMR spectroscopy, which was identical to the authentic compound.



Scheme 21. The mechanism of the S-oxidation of Et 770

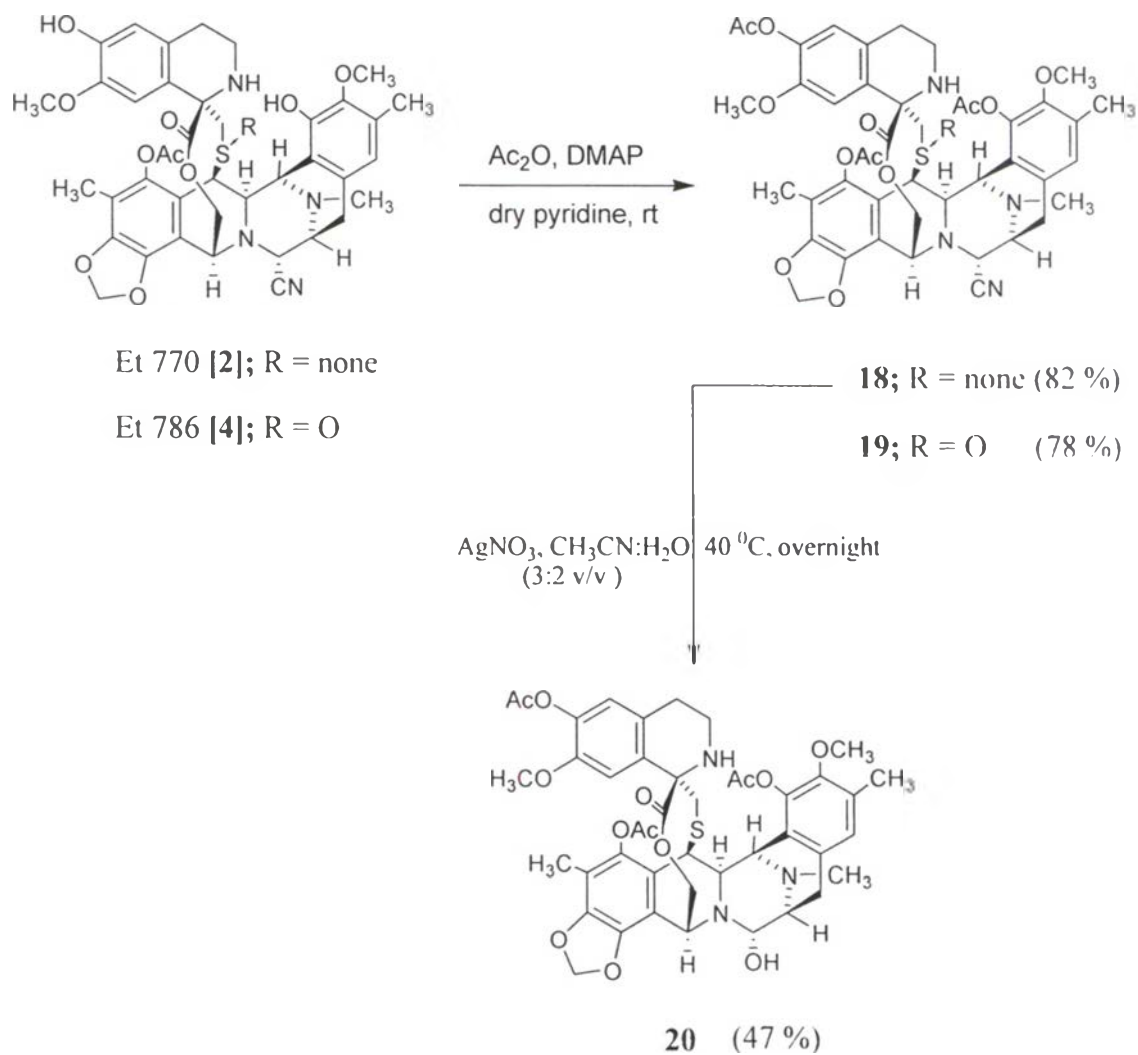
2.2 Preparation of ecteinascidin analogs

2.2.1 Preparation of acetate ester analogs

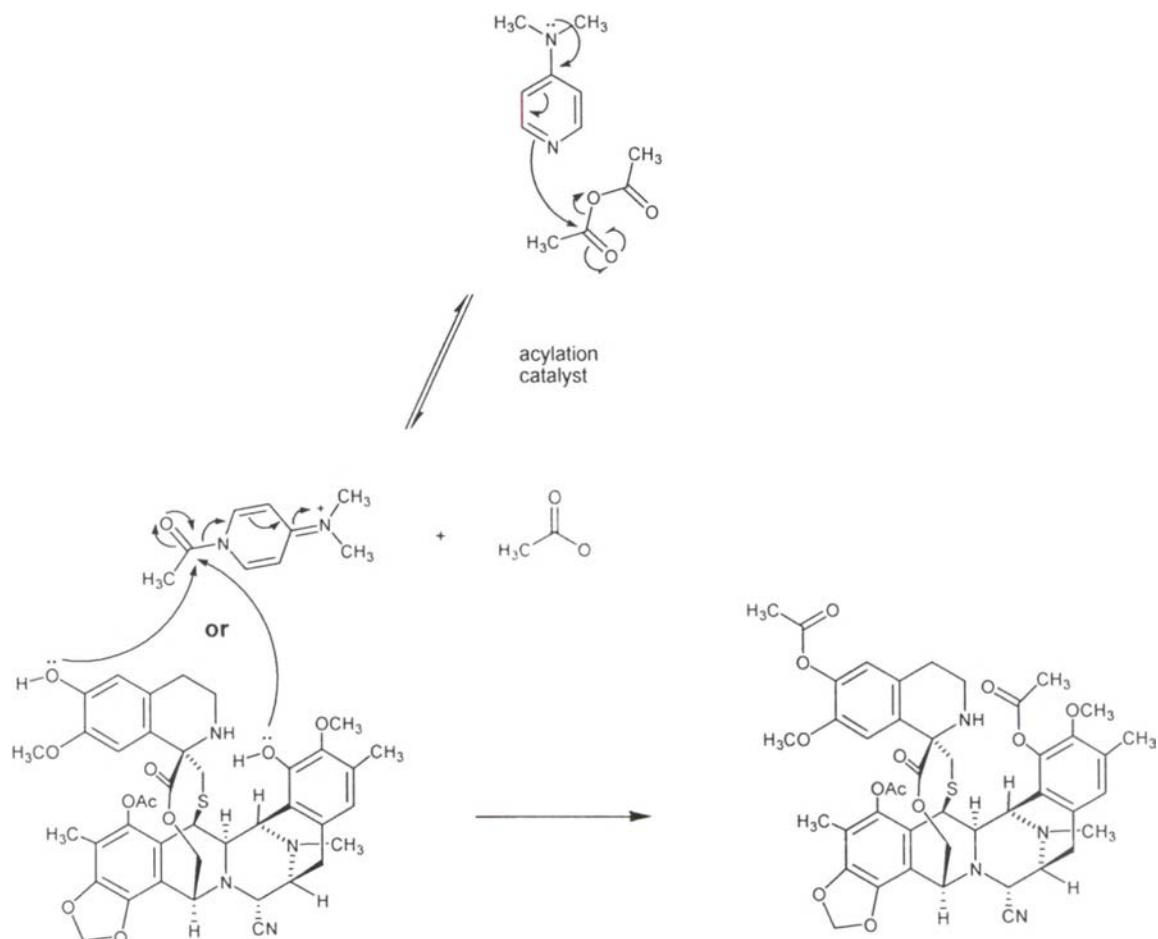
Previous results suggested that the *A*- and *B*-subunits of the ecteinascidin-type are the critical structure for DNA recognition and bonding in the minor groove of DNA, while the *C*-subunit is protruded out of the minor groove of DNA (Pommier *et al.*, 1996; Moore *et al.*, 1997; 1998; Takebayashi *et al.*, 1999; Zewail-Foote *et al.*, 1999). However, the role of the *C*-subunit on cytotoxic activity of ecteinascidin compounds is unclear. In addition, there are other factors such as duplex stabilization and extrahelical protrusion of the *C*-subunit, which has conformational flexibility, that may also contribute to the clinical effectiveness of the ecteinascidins. As previously described, the successful isolation of Et 770 and Et 786 in high yield from the Thai tunicate, *Ecteinascidia thrustoni*, has led us to study the effects of the *C*-subunit on the cytotoxicity. Therefore, analogs preparation at the phenolic hydroxyl in the *C*-subunit of Et 770 and Et 786 and their cytotoxic activities are investigated in this study.

Both phenolic hydroxyl groups on the *A*- and *C*-subunits of Et 770 and Et 786 can be easily transformed to 18,6'-diacetates of Et 770 (**18**) and Et 786 (**19**), respectively, with acetic anhydride in the presence of catalytic amount of 4-dimethyl aminopyridine (DMAP) and pyridine at room temperature as shown in Scheme 22 and the proposed

mechanism is outline in Scheme 23. The α -cyano amine of **18** can be converted to the α -hydroxyl amine by silver nitrate to afford 18,6'-diacetate of Et 743 (**20**).



Scheme 22. Preparative scheme of diacetate ester analogs of the ecteinascidins



Scheme 23. The proposed reaction mechanism of esterification reaction.

High-resolution FABMS of **18** showed the pseudo-molecular ion ($M + H$)⁺ peak at m/z 855.2913 which is corresponding to the molecular formula $C_{44}H_{47}N_4O_{12}S$ (calcd. 855.2911). The 84 mass units higher than Et 770 indicated that the diacetate ester was obtained. The chemical structure of **18** was mainly analyzed by NMR spectroscopy. ¹H and ¹³C-NMR spectra of **18** showed the most characteristic signals similar to those of Et 770. The NMR signals of two acetoxy groups in **18** appeared as follows: the methyl signals at δ_H 2.24 and 2.37, δ_C 20.6 ppm; the carbonyl carbons at δ_C 167.9 and 169.0 ppm. In addition, the ¹H-NMR spectra data of **18** lacked the signals of 18-OH and 6'-OH compared to those of Et 770 at δ 5.77 and 5.97 ppm, respectively, suggesting both phenolic hydroxyls were substituted with the acetyl groups. Furthermore, the carbon signals of C-15 and C-19 in the *A*-subunit were shifted downfield to δ 127.3 and 124.3

ppm, respectively and also C-9' in the C'-subunit to δ 132.3 ppm, which were shifted downfield about 6 ppm. In addition, C-5' and C-7' in the C'-subunit were also downfield shifted about 8.4 ppm and 3.8 ppm, respectively compared with the original signals of Et 770 (Figure 15 and Table 12). The partial NMR data of **2** and **18** are shown in Table 12. Since ortho and para aromatic carbons are interfered from anisotropic effects resulting downfield shifts. It was consequently suggested the ester bond linkage on phenolic hydroxyl at the A- and C'-subunits.

Based on data of **18**: ecteinascidin 786 18.6'-diacetate (**19**) and ecteinascidin 743 18.6'-diacetate (**20**) were identical to those diacetate ester analogs on phenolic hydroxyl groups at the A- and C'-subunits. Their structures were mainly determined from HR-FABMS and $^1\text{H-NMR}$ data: ecteinascidin 786 18.6'-diacetate (**19**) presented a pseudo-molecular ion $(\text{M} + \text{H})^+$ peak at m/z 871.2852 corresponding to the molecular formula $\text{C}_{44}\text{H}_{47}\text{N}_4\text{O}_{13}\text{S}$ (Calcd. 871.2860) and ecteinascidin 743 18.6'-diacetate (**20**) resulted a fragment ion $[\text{M} + \text{H} - \text{H}_2\text{O}]^+$ peak at m/z 828.2800 (calcd for $\text{C}_{43}\text{H}_{46}\text{N}_3\text{O}_{12}\text{S}$, 828.2802).

Et 770

Ecteinascidin 770 18,6'-diacetate

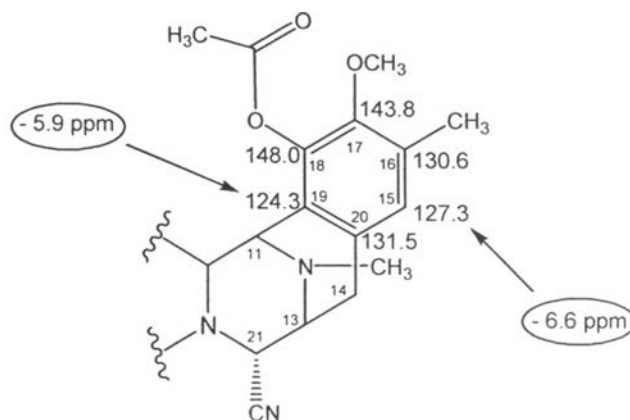
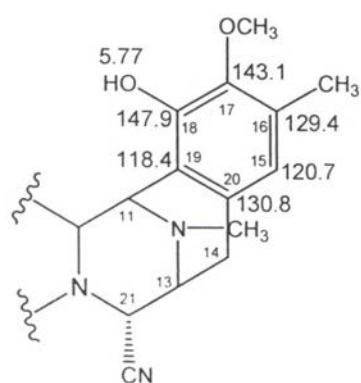
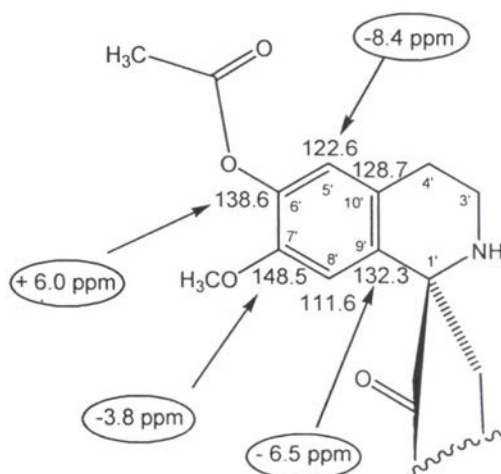
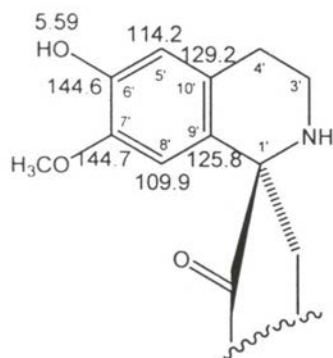
A-subunit*C*-subunit

Figure 15. Partial ¹H and ¹³C-NMR assignment data of the *A*- and *C*-subunits of Et 770 (**2**) and Ecteinascidin 770 18,6'-diacetate [**18**]

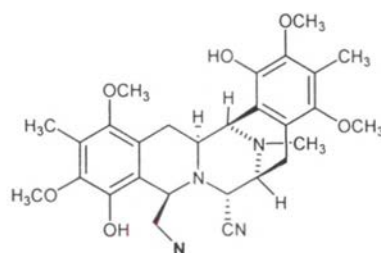
Table 12. ^1H and ^{13}C -NMR spectra data of Et 770 [2] and Et 770 18,6'-diacetate [18] recorded in CDCl_3

Positions	Et 770 18, 6'-diacetate [18]		Et 770 [2]	
	δ_{H} J (Hz)	δ_{C}	δ_{H} J (Hz)	δ_{C}
1	4.34 s	61.1	4.32 s	61.2
3	3.52 d (4.6)	59.6	3.51 d (4.9)	59.7
4	4.44 br s	42.1	4.57	41.9
5		141.3		141.4
6		113.6		113.4
7		145.6		145.3
8		140.4		140.2
9		113.9		114.1
10		120.8		121.2
11	3.83 d (4.6)	55.8	4.28 dd (4.9, 1.2)	54.8
13	3.46 dt (4.9, 2.8)	54.4	3.41 br t	54.7
14	2.99 d (4.9)	24.0	2.91 d (7.6)	24.2
15	6.95 s	127.3	6.60 s	120.7
16		130.6		129.4
17		143.8		143.1
18		148.0		147.9
19		124.3		118.4
20		131.5		130.8
21	4.18 d (2.8)	59.2	4.18 d (2.8)	59.6
22	5.02 d (11.3)	60.1	5.01 d (11.6)	60.1
	4.12 dd (11.3, 2.2)		4.12 dd (11.6, 2.0)	
23	6.04 s	102.0	6.04 d (1.2)	102.0
	5.98 s		5.97 d (1.2)	
1'		65.0		64.9
3'	3.12 m	39.6	3.11 m	39.7
	2.83 m		2.79 m	
4'	2.65 m	28.5	2.60 m	28.8
	2.49 m		2.42 dt (15.9, 3.4)	
5'	6.62 s	122.6	6.46 s	114.2
6'		138.6		144.6
7'		148.5		144.7
8'	6.54 s	111.6	6.44 s	109.9
9'		132.3		125.8
10'		128.7		129.2
11'		172.0		172.6
12'	2.33 br d	42.4	2.35 br d	42.3
	2.24 br d		2.15 br d	
21-CN		117.8		118.7
N-CH ₃	2.16 s	41.5	2.19 s	41.6
6-CH ₃	2.04 s	9.6	2.04 s	9.7
16-CH ₃	2.33 s	15.8	2.32 s	15.8
17-OCH ₃	3.72 s	60.1	3.78 s	60.4
7'-OCH ₃	3.56 s	55.6	3.60 s	55.2
5-OCOCH ₃	2.30 s	20.2	2.26 s	20.4
5-OCOCH ₃		167.9		168.2
18-OCOCH ₃	2.24 (2.37) s	20.6		
18-OCOCH ₃		167.9 (169.0)		
6'-OCOCH ₃	2.37 (2.24) s	20.6		
6'-OCOCH ₃		169.0 (167.9)		
18-OH			5.77 s	
6'-OH			5.59 s	

2.2.2 Preparation of aromatic ester analogs

Previously, Corey and Martinez have reported the discovery of the structurally simple molecule phthalascidin, which was exploited from the synthetic route to the ecteinascidins. Although, phthalascidin contained an α -cyanoamine functionality, but it was surprisingly found to have comparable biological activity to Et 743 (Table 5), which is in contrast to the case of saframycin A, a bisquinone alkaloid obtained an α -cyanoamine group. Lately, saframycin A analogs were prepared by amide bond forming and the biological activities were assayed using two human cancer cell lines, A375 melanoma and A549 lung carcinoma, are outlined in Table 13 (Myers *et al.*, 2001; 2002).

Table 13. Some of the most potent bishydroquinone derivatives of saframycin A and their antiproliferative activity



N	IC ₅₀ , nM		N	IC ₅₀ , nM	
	A375	A549		A375	A549
Saframycin A	5.3	133		2.7	31
	4.5	160		1.7	9.2
	13	290		3.3	40
	2.4	39		2.5	32
	2.5	37		1.3	4.4
	1.4	14		1.4	4.6
	1.2	11		2.0	3.5
	1.2	6.5		1.5	4.1
	1.7	25		1.2	4.7
	1.9	37		3.6	78

The pentacyclic natural products, such as saframycins and renieramycins occurred from the condensation between the *A*- and *B*-subunits to structure with shape as propeller-like character. Both of which are fairly flat molecules when compared to ecteinascidin molecule (Scott, *et al.* 2002). However, the extra *C*-subunit is perpendicular to the combined *AB*-subunit (Sakai *et al.*, 1992; Sainz-Diaz *et al.*, 2003), suggesting that the condensation between three large principal planar groups to case molecule shape is highly compact. Therefore, the phenolic hydroxyl in the *C*-subunit hardly appeared steric hindrance, while the phenolic hydroxyl in the *A*-subunit was subjected to that steric from the ten-membered lactone ring and also the *C*-subunit molecule (Figure 16). Therefore, substitution on phenolic hydroxyl of the *C*-subunit can reactively occur much more easier than the *A*-subunit. Therefore, bulky acylation will be selected on the phenolic hydroxyl at the *C*-subunit.

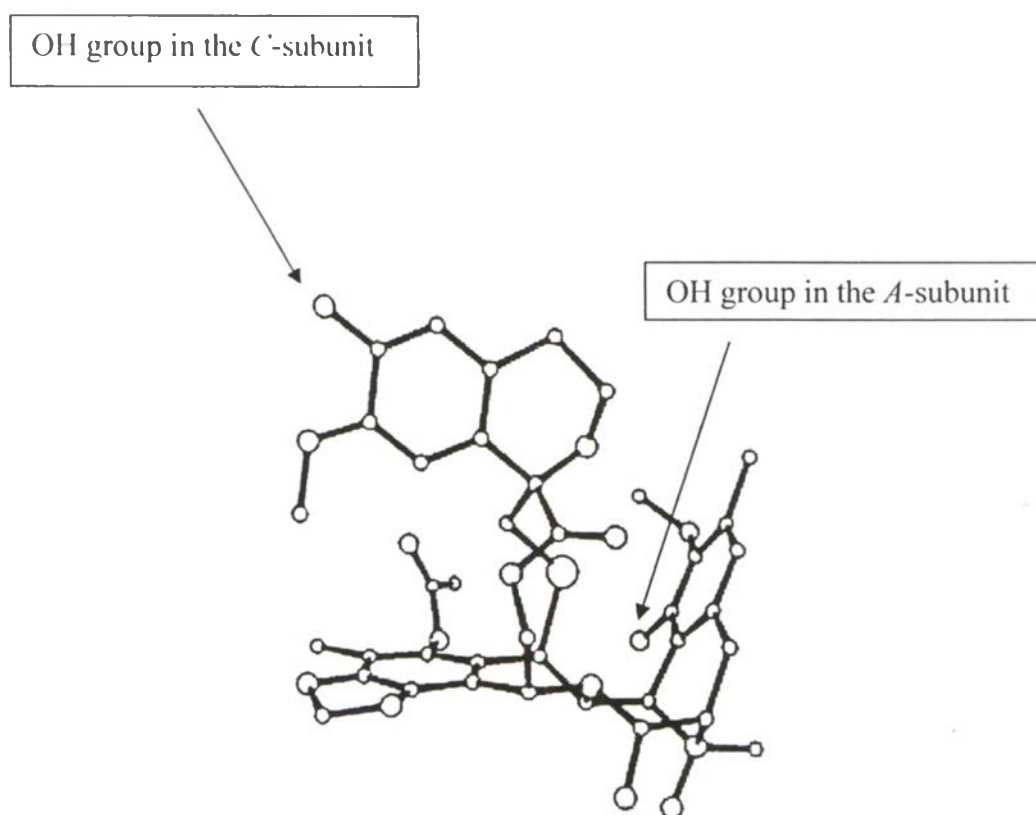


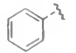
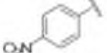
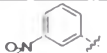
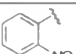
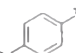
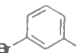
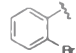
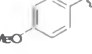
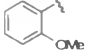
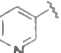

Figure 16. 3D-structure of ecteinascidin molecule

Since Et 770 can be easily transformed to Et 743 in high yield. Thus, other derivatives of Et 743 can be prepared through Et 770 concept. Our attention was focused on the synthetic study of several types of bulky aromatic acid ester derivatives at the C-subunit. Therefore, a variety of aromatic acid such as benzoyl (**15**), substituted benzoyl (**16-23**), pyridinoyl (**24-25**), naphthoyl (**26-27**), quinolinoyl (**28-29**), isoquinolinoyl (**30-31**) will be prepared in this study as shown in Table 1. In contrast with the acetylation as above, Et 770 was treated with the corresponding acid chlorides and catalytic amount of DMAP in the presence of pyridine to afford mainly monoacyl derivatives **15-29** in 66-96% yields (Table 14).

As described above, compounds **21-33** were prepared from available acid chlorides, while the preparations of **34** and **35** began from conversion of available quinoline carboxylic acids with thionyl chloride to result quantitative quinoline carboxyl chloride. Resulting acid chloride was further reacted with Et 770 following to the above procedure to afford monoacyl derivatives **34** and **35** in 98% and 96% yields (Table 14), respectively.

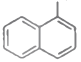
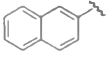
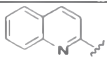
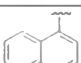
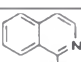
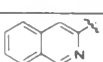
In addition, the commercially available isoquinoline 1- and 3-carboxylic acids were first converted to their corresponding acid chlorides as reagents for compounds **36** and **37**, respectively. Unfortunately, the similar acylation methods with the corresponding acid chlorides to prepare the isoquinolinoyl derivatives were unsuccessful. However, it might be the case that the isoquinoline carboxyl chlorides were not obtained in this condition. Thus, the coupling reactions were carried on acylation of isoquinoline carboxylic acid with Et 770 in the presence of dicyclohexyl carbodiimide (DCC) in dichloromethane at room temperature for overnight. Unfortunately, **36** and **37** were obtained in poor yields (12% and 24 %, respectively). The proposed mechanism of reaction is depicted in Scheme 24.

Table 14. Summary of yields. High-resolution FABMS data and methods for the prepared monoacyl derivatives of Et 770

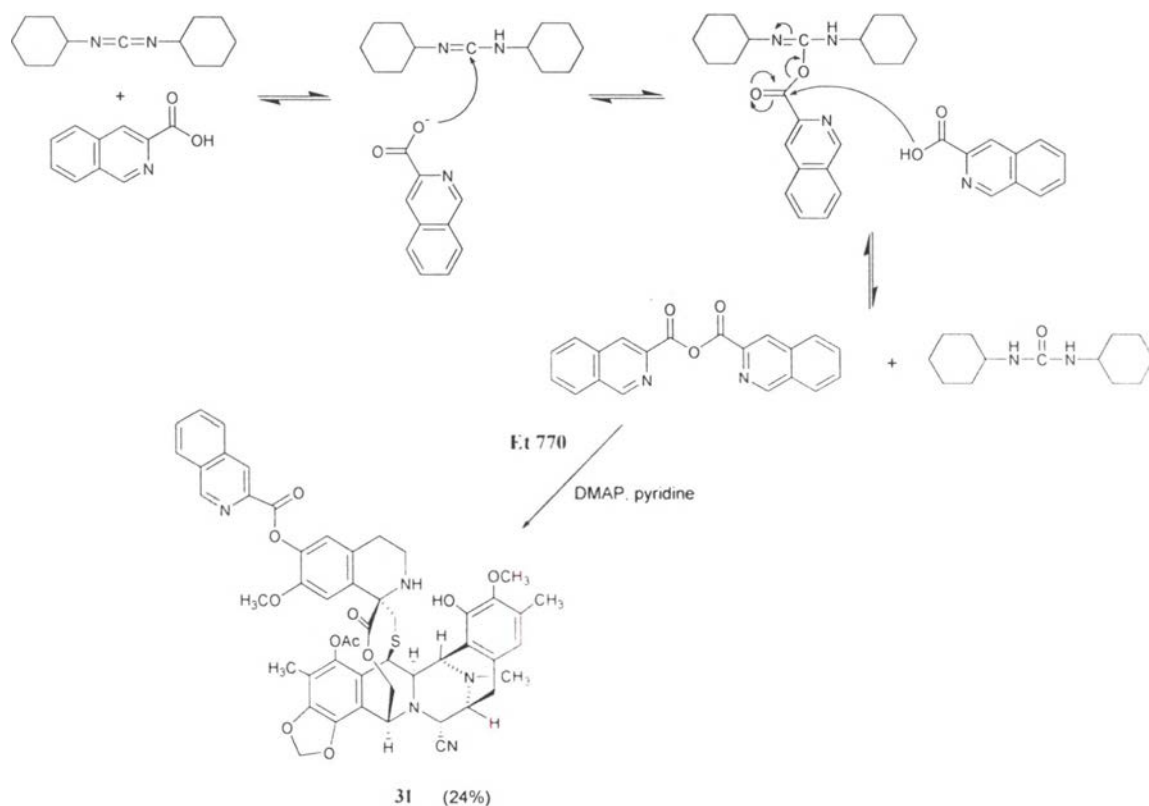
Cpds	Ar	condition (% yield)	molecular formula	<i>m/z</i> (HR-FABMS)Calcd.	optical rotation (in CHCl ₃)
15		a (88)	C ₄₇ H ₄₆ N ₄ O ₁₁ S	875.2964 [M + H] ⁺ , calcd for C ₄₇ H ₄₇ N ₄ O ₁₁ S, 875.2962	[α] _D ²² -20.2 ⁰ (c 0.33)
16		a (95)	C ₄₇ H ₄₅ N ₅ O ₁₃ S	920.2824 [M + H] ⁺ , calcd for C ₄₇ H ₄₆ N ₅ O ₁₃ S, 920.2812	[α] _D ²⁰ -28.8 ⁰ (c 0.68)
17		a (66)	C ₄₇ H ₄₅ N ₅ O ₁₃ S	920.2831 [M + H] ⁺ , calcd for C ₄₇ H ₄₆ N ₅ O ₁₃ S, 920.2812	[α] _D ²⁰ -18.5 ⁰ (c 0.21)
18		a (83)	C ₄₇ H ₄₅ N ₅ O ₁₃ S	920.2811 [M + H] ⁺ , calcd for C ₄₇ H ₄₆ N ₅ O ₁₃ S, 920.2812	[α] _D ¹⁹ -17.8 ⁰ (c 0.15)
19		a (97)	C ₄₇ H ₄₅ N ₄ O ₁₁ BrS	953.2057 [M + H] ⁺ , calcd for C ₄₇ H ₄₆ N ₄ O ₁₁ BrS, 953.2067 FAB-MS; 955[M + 2+ H] ⁺ , 953 [M + H] ⁺	[α] _D ¹⁹ -30.9 ⁰ (c 0.75)
20		a (84)	C ₄₇ H ₄₅ N ₄ O ₁₁ BrS	953.2018 [M + H] ⁺ , calcd for C ₄₇ H ₄₆ N ₄ O ₁₁ BrS, 953.2067 FAB-MS; 955[M + 2+ H] ⁺ , 953 [M + H] ⁺	[α] _D ²¹ -17.9 ⁰ (c 0.14)
21		a (74)	C ₄₇ H ₄₅ N ₄ O ₁₁ BrS	953.2080 [M + H] ⁺ , calcd for C ₄₇ H ₄₆ N ₄ O ₁₁ BrS, 953.2067 FAB-MS; 955[M + 2+ H] ⁺ , 953 [M + H] ⁺ 67	[α] _D ²¹ -44.9 ⁰ (c 0.17)
22		a (67)	C ₄₈ H ₄₈ N ₄ O ₁₂ S	905.3058 [M + H] ⁺ , calcd for C ₄₈ H ₄₉ N ₄ O ₁₂ S, 905.3068	[α] _D ²⁰ -34.8 ⁰ (c 0.27)
23		a (72)	C ₄₈ H ₄₈ N ₄ O ₁₂ S	905.3074 [M + H] ⁺ , calcd for C ₄₈ H ₄₉ N ₄ O ₁₂ S, 905.3068	[α] _D ¹⁹ -48.2 ⁰ (c 0.85)
24		a (76)	C ₄₆ H ₄₅ N ₅ O ₁₁ S	876.2911 [M + H] ⁺ , calcd for C ₄₆ H ₄₆ N ₅ O ₁₁ S, 876.2914	[α] _D ¹⁷ -33.7 ⁰ (c 0.45)
25		a (85)	C ₄₆ H ₄₅ N ₅ O ₁₁ S	876.2921 [M + H] ⁺ , calcd for C ₄₆ H ₄₆ N ₅ O ₁₁ S, 876.2914	[α] _D ²⁰ -38.7 ⁰ (c 0.45)

Conditions: a) ArCOOCl, Ac₂O, DMAP, dry pyridine, rt, 4 h. - overnight. b) ArCOOH, DCC, CH₂Cl₂, rt, overnight. c) ArCOOCOOCH(CH₃)₂, Ac₂O, DMAP, dry pyridine, rt, overnight.

Table 14. (Continued)

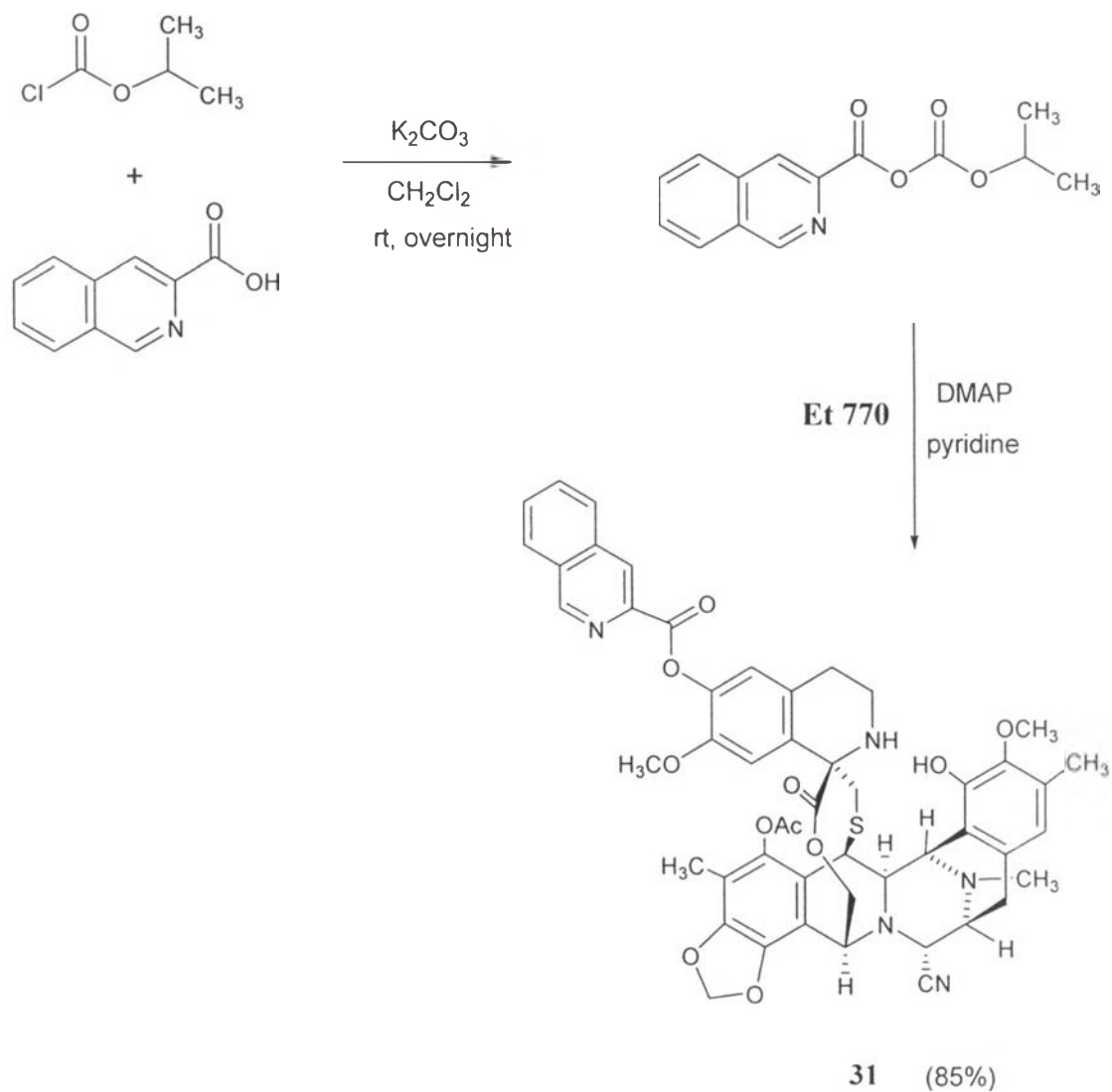
Cpds	Ar	condition (% yield)	molecular formula	<i>m/z</i> (HR-FABMS)Calcd.	optical rotation (in CHCl ₃)
26		a (96)	C ₅₁ H ₄₈ N ₄ O ₁₁ S	925.3128 [M + H] ⁺ , calcd for C ₅₁ H ₄₉ N ₄ O ₁₁ S, 925.3118	[α] _D ²⁰ -55.4 ⁰ (c 0.17)
27		a (94)	C ₅₁ H ₄₈ N ₄ O ₁₁ S	925.3125 [M + H] ⁺ , calcd for C ₅₁ H ₄₉ N ₄ O ₁₁ S, 925.3118	[α] _D ²⁰ -22.6 ⁰ (c 0.62)
28		a (99)	C ₅₀ H ₄₇ N ₅ O ₁₁ S	926.3079 [M + H] ⁺ , calcd for C ₅₀ H ₄₈ N ₅ O ₁₁ S, 926.3021	[α] _D ²¹ -21.0 ⁰ (c 0.17)
29		a (96)	C ₅₀ H ₄₇ N ₅ O ₁₁ S	926.3079 [M + H] ⁺ , calcd for C ₅₀ H ₄₈ N ₅ O ₁₁ S, 926.3021	[α] _D ²¹ -25.3 ⁰ (c 0.17)
30		b (12) c (70)	C ₅₀ H ₄₇ N ₅ O ₁₁ S	926.3083 [M + H] ⁺ , calcd for C ₅₀ H ₄₈ N ₅ O ₁₁ S, 926.3021	[α] _D ²² -36.1 ⁰ (c 0.43)
31		b (24) c (85)	C ₅₀ H ₄₇ N ₅ O ₁₁ S	926.3081 [M + H] ⁺ , calcd for C ₅₀ H ₄₈ N ₅ O ₁₁ S, 926.3021	[α] _D ²¹ -35.6 ⁰ (c 0.45)

Conditions: a) ArCOOCl, Ac₂O, DMAP, dry pyridine, rt, 4 h. - overnight. b) ArCOOH, DCC, CH₂Cl₂, rt, overnight. c) ArCOOCOOCH(CH₃)₂, Ac₂O, DMAP, dry pyridine, rt, overnight.



Scheme 24. The proposed mechanism of acylation of isoquinolinoyl derivatives *via* DCC coupling reagent

In order to improve the yields of the isoquinolinoyl derivatives, the available isoquinoline carboxylic acids were converted to the anhydride reagents. Treatment of the available carboxylic acid with isopropyl chloroformate and anhydrous potassium carbonate (K_2CO_3) was carried in dry dichloromethane at room temperature for overnight to give quantitative amount of the anhydride reagents. Resulting anhydride without purification was immediately used in the next step with the general procedure as described to afford **36** and **37** with 69 % and 85 % yields, respectively (Scheme 25).



Scheme 25. Preparation of isoquinolinoyl derivatives *via* anhydride reagent

The structures of the synthesized ecteinascidin analogs were elucidated predominantly by the interpretation of NMR and MS data. Assignments for all protons and carbons of the compounds were mainly accomplished by extensive analyses through 1D-NMR and 2D-NMR measurements, including H-H COSY, HMQC, HMBC and NOESY techniques.

The HR-FABMS spectral data of all synthesized aromatic ester derivatives confirmed that the ecteinascidin was mono-acylated. Almost of mass spectra obtained the $[M + H]^+$ ion (Table 13), together with the major fragment ions at m/z 204, 206, 218, 243 and 245 as shown in Figure 17. These fragment ions suggested that the phenolic hydroxyl in the *A*-subunit was not acylated.

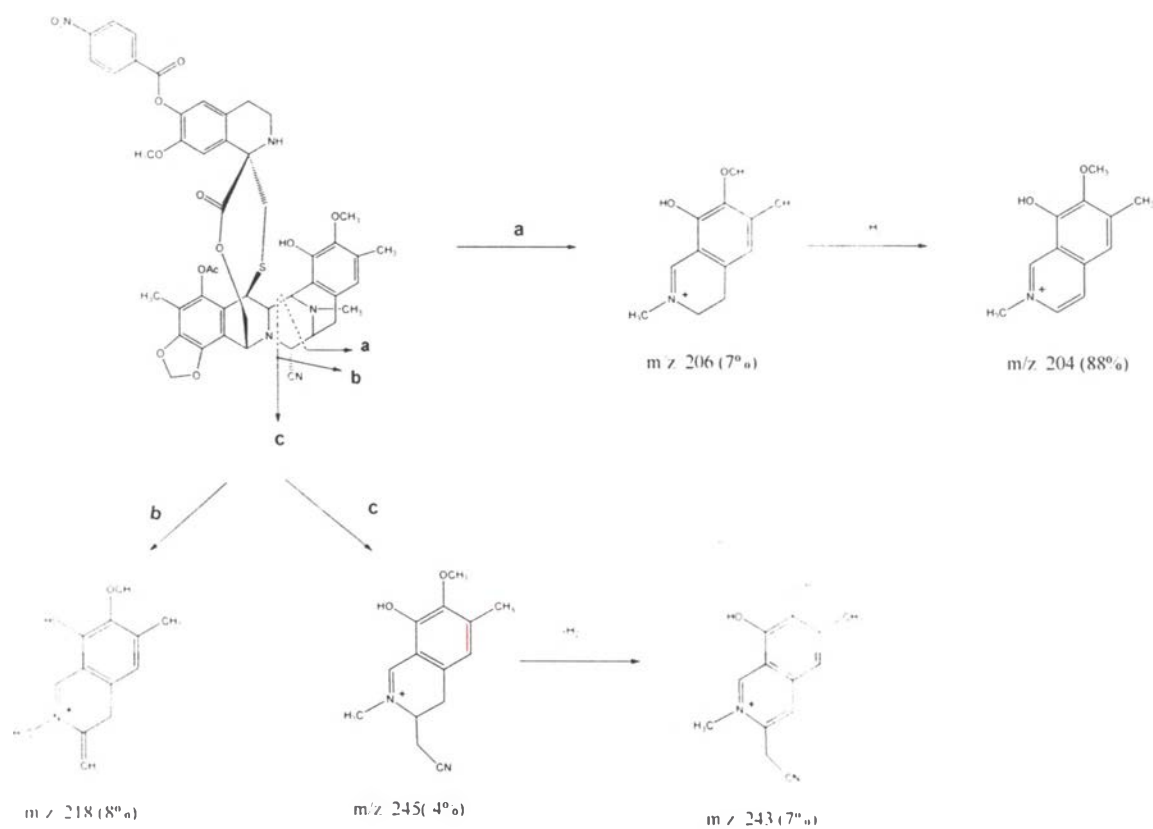
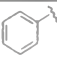
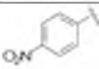
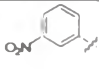
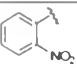
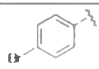
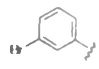
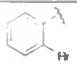
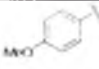
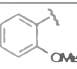
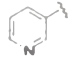


Figure 17. The proposed FABMS fragment ions pattern of Ecteinascidin 770 6'-O-4''-nitrobenzoate (22)

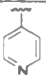
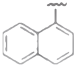
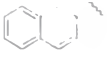
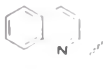
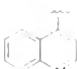
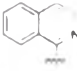
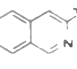
The mono acylation at C-6' in the C'-subunit was proven based on NMR measurement. The NMR data of the aroyl substituents (**21-37**) are presented in Table 15. The ^1H -NMR signals attributable to the benzoyl, substituted benzoyl, quinolinoyl, isoquinolinoyl, naphthoyl and pyridinoyl are in the range of δ 6.95-9.38 ppm and also for the ^{13}C -NMR signals in the range of δ 110-155 ppm.

Table 15. ^1H - and ^{13}C -NMR spectral data of the acyl moieties of the aroyl substituted Et 770 derivatives (**21-37**)

Cpds	Substituent	NMR assignments	
		δ_{H} J (Hz)	δ_{C}
21		8.14 (2H, d, $J = 8.4$ Hz), 7.60 (1H, t, $J = 8.4$ Hz), 7.47 (2H, t, $J = 8.4$ Hz)	ND
22		8.31 (4H, s, Ar-H)	150.8, 134.7, 131.3 (2C), 123.6 (2C)
23		8.96 (1H, t, $J = 1.8$ Hz), 8.45 (2H, dd, $J = 8.1, 1.8$ Hz), 7.69 (1H, t, $J = 8.1$ Hz)	ND
24		7.92 (1H, d, $J = 8.9$ Hz), 7.88 (1H, d, $J = 7.4$ Hz), 7.72 (2H, m)	ND
25		7.99 (2H, d, $J = 8.5$ Hz), 7.61 (2H, d, $J = 8.5$ Hz)	131.8 (2C), 131.7 (2C), 131.4, 128.2
26		8.27 (1H, t, $J = 2.0$ Hz), 8.06 (1H, d, $J = 8.1$ Hz), 7.73 (1H, dd, $J = 8.1, 2.0$ Hz), 7.35 (1H, t, $J = 8.1$ Hz)	ND
27		8.00 (1H, m), 7.70 (1H, m), 7.38 (2H, m)	ND
28		8.09 (2H, d, $J = 8.6$ Hz), 6.95 (2H, d, $J = 8.6$ Hz), 3.87 (3H, s, 4''-OCH ₃)	ND
29		7.98 (1H, dd, $J = 8.2, 1.5$ Hz), 7.51 (1H, dt, $J = 8.2, 1.5$ Hz), 7.00 (2H, t, $J = 8.2$ Hz), 3.89 (3H, s, 4''-OCH ₃)	159.9, 135.0, 132.4, 120.2 (2C), 112.3, 56.0
30		9.29 (1H, dd, $J = 2.2, 0.6$ Hz), 8.80 (1H, dd, $J = 4.9, 1.8$ Hz), 8.34 (1H, ddd, $J = 7.9, 2.2, 1.8$ Hz), 7.40 (1H, ddd, $J = 7.9, 4.9, 0.6$ Hz)	153.8, 151.5, 137.4, 125.4, 123.4

ND = not detected

Table 15. (Continued)

Cpds	Substituent	NMR assignments	
		δ_{H} J (Hz)	δ_{C}
31		8.80 (2H, dd, $J = 4.5, 1.5$ Hz), 7.92 (2H, dd, $J = 4.5, 1.5$ Hz)	150.7 (2C), 136.6, 123.3 (2C)
32		8.94 (1H, d, $J = 8.3$ Hz), 8.37 (1H, dd, $J = 7.3, 1.3$ Hz), 8.06 (1H, d, $J = 8.1$ Hz), 7.89 (1H, dd, $J = 7.9, 1.5$ Hz), 7.61 (1H, m), 7.58 (1H, m), 7.55 (1H, dd, $J = 8.1, 7.3$ Hz)	ND
33		8.73 (1H, br s), 8.11 (1H, dd, J $= 8.6, 1.5$ Hz), 7.97 (1H, d, $J =$ 7.9 Hz), 7.91 (1H, d, $J = 8.6$ Hz), 7.89 (1H, d, $J = 7.9$ Hz), 7.61 (1H, dt, $J = 8.6, 1.5$ Hz), 7.54 (1H, dt, $J = 8.5, dt, J =$ 8.6, 0.9 Hz)	135.8, 132.5, 132.0, 129.5, 128.5, 128.3 (2C), 127.8, 126.7, 125.6
34		8.34 (1H, d, $J = 8.4$ Hz), 8.33 (1H, d, $J = 8.3$ Hz), 8.25 (1H, d, $J = 8.4$ Hz), 7.90 (1H, d, $J =$ 8.1 Hz), 7.80 (1H, dd, $J = 8.3,$ 7.7 Hz), 7.67 (1H, dd, $J = 8.1,$ 7.7 Hz)	ND
35		9.07 (1H, d, $J = 4.6$ Hz), 8.80 (1H, dd, $J = 8.5, 1.5$ Hz), 8.19 (1H, dd, $J = 8.5, 0.6$ Hz), 8.07 (1H, d, $J = 4.3$ Hz), 7.79 (1H, ddd, $J = 8.5, 7.0, 1.5$ Hz), 7.65 (1H, ddd, $J = 8.5, 7.0, 1.5$ Hz)	149.8, 149.1, 34.0, 130.0, 129.8, 28.4, 125.6, 125.2, 122.8
36		δ : 8.86 (1H, d, $J = 8.5$ Hz), 8.67 (1H, d, $J = 5.5$ Hz), 7.90 (1H, d, $J = 8.2$ Hz), 7.86 (1H, d, $J = 5.5$ Hz), 7.74 (1H, dt, $J =$ 8.5, 1.1 Hz), 7.68 (1H, dt, $J =$ 8.5, 1.4 Hz)	147.8, 141.8, 37.0, 130.5, 128.8, 127.2, 127.1, 126.4, 124.4
37		9.38 (1H, s), 8.69 (1H, s), 8.08 (1H, d, $J = 7.9$ Hz), 8.00 (1H, d, $J = 7.9$ Hz), 7.80 (1H, dt, $J =$ 7.9, 1.2 Hz), 7.70 (1H, dt, $J =$ 7.9, 0.6 Hz)	152.9, 140.8, 135.4, 131.2, 130.1, 129.8, 128.1, 127.7, 125.0,

ND = not detected

Herein, Ecteinascidin 770 6'-O-4''-nitrobenzoate (**22**) was chosen to demonstrate the acylation occurring at the phenolic hydroxyl in the C'-subunit. The signals of C-5', C-7' and C-9' were shifted downfield to δ 122.3 ppm, δ 148.3 ppm, and δ 133.2 ppm, respectively [C-5' (δ 114.2 ppm), C-7' (δ 144.7 ppm) and C-9' (δ 125.8 ppm) of **2**]. The signal of C-6' was shifted upfield to δ 138.6 ppm compared with that of **2** (δ 144.6 ppm) (Figure 18 and Table 16).

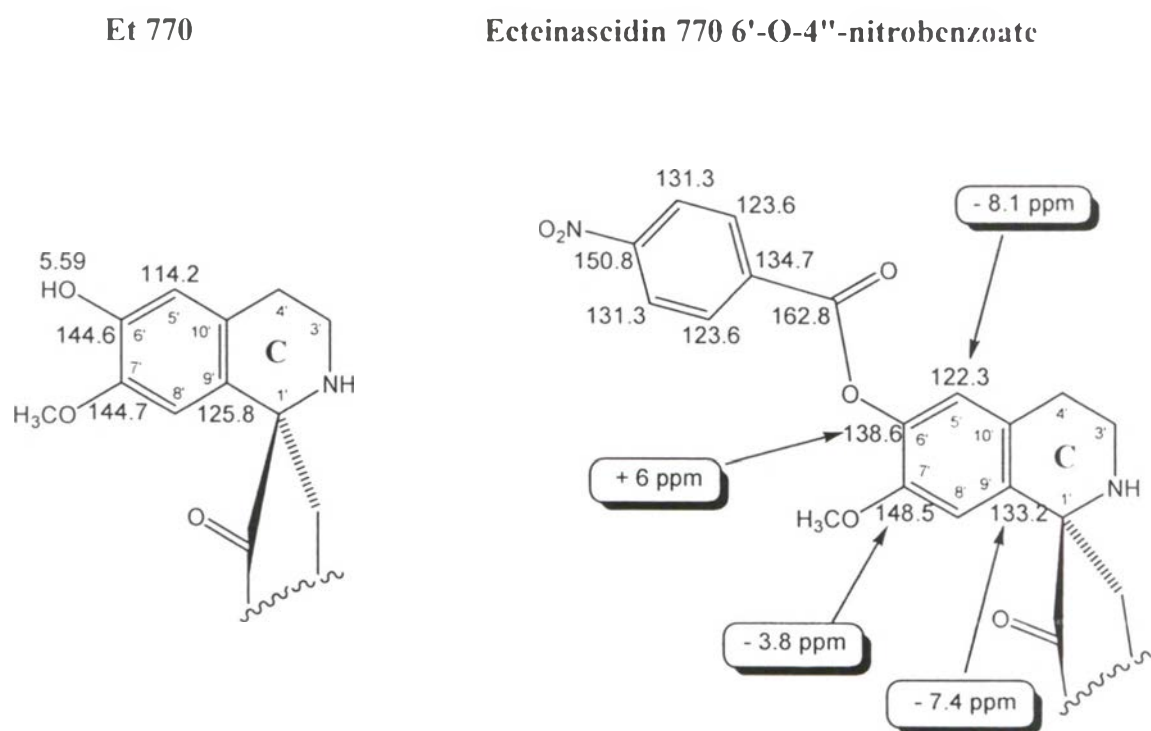


Figure 18. Partial ^{13}C -NMR assignment data in the C'-subunit of Ecteinascidin 770 6'-O-4''-nitrobenzoate (**22**)

Furthermore, the signal of un-substituted phenolic hydroxyl proton at C-18 of the *A*-subunit represented the chemical shift at δ 5.76 ppm and showed NOESY correlation with 17-OCH₃ (Figure 19 and 46). Moreover, carbon signals of C-15, C-17, C-18 and C-19 at the *A*-subunit displayed the identical chemical shift to those the *A*-subunit of starting material (**2**). In addition, the characteristic of FABMS fragment ions at m/z 204, 206, 218, 243 and 245 were also represented (Figure 17). These observation confirmed that the free OH group is at C-18 of **22**. The above mentioned information revealed 6'-*O*-acylation in **22** and the structural elucidation of those ecteinascidin analogs (**21** and **23-37**) were all in similar manner to that of **22**.

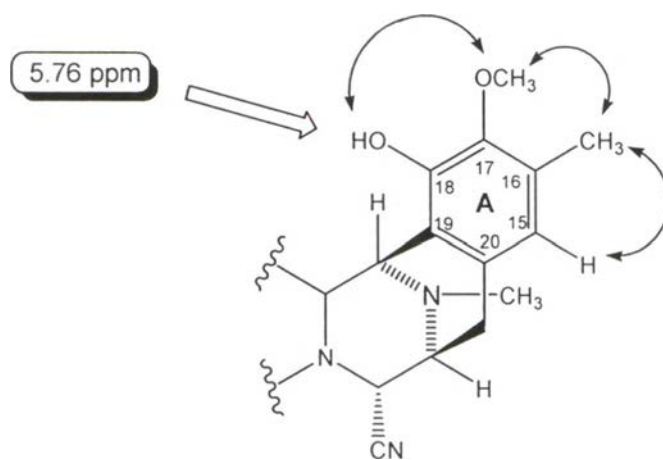
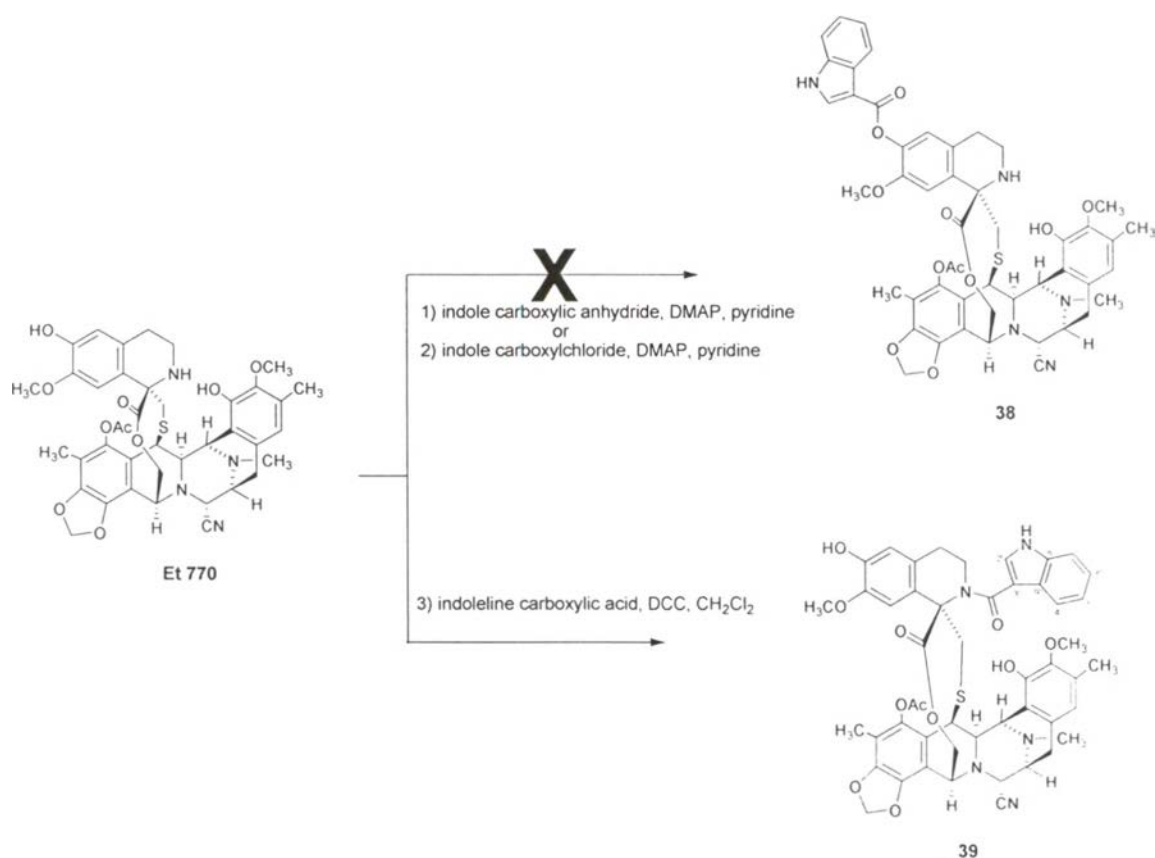


Figure 19. Partial correlations observed in the NOESY (\leftrightarrow) spectrum of Ecteinascidin 770 6'-*O*-4''-nitrobenzoate (**22**) in the *A*-subunit

Table 16. Partial ^1H and ^{13}C -NMR spectra data of the core structures of Et 770 [2] and Ecteinasidin 770 6'-*O*-4"-nitrobenzoate [22] recorded in CDCl_3

Positions	22		Et 770 [2]	
	$\delta_{\text{H}} J$ (Hz)	δ_{C}	$\delta_{\text{H}} J$ (Hz)	δ_{C}
1	4.35 s	61.1	4.32 s	61.2
3	3.53 d (4.6)	59.6	3.51 d (4.9)	59.7
4	4.59 br s	42.0	4.57	41.9
5		141.4		141.4
6		113.5		113.4
7		145.4		145.3
8		140.1		140.2
9		114.0		114.1
10		121.0		121.2
11	4.29 d (3.7)	54.7	4.28 dd (4.9, 1.2)	54.8
13	3.43 br t	54.6	3.41 br t	54.7
14	2.96 d (6.1)	24.2	2.91 d (7.6)	24.2
15	6.61 s	120.7	6.60 s	120.7
16		129.4		129.4
17		143.1		143.1
18		147.9		147.9
19		118.2		118.4
20		130.8		130.8
21	4.19 d (2.7)	59.6	4.18 d (2.8)	59.6
22	5.04 d (11.6)	60.2	5.01 d (11.6)	60.1
	4.14 dd (11.6, 2.2)		4.12 dd (11.6, 2.0)	
23	6.02 d (0.9)	101.9	6.04 d (1.2)	102.0
	5.96 d (0.9)		5.97 d (1.2)	
1'		64.9		64.9
3'	3.15 m	39.5	3.11 m	39.7
	2.83 m		2.79 m	
4'	2.67 m	29.6	2.60 m	28.8
	2.52 m		2.42 dt (15.9, 3.4)	
5'	6.75 s	122.3	6.46 s	114.2
6'		138.6		144.6
7'		148.3		144.7
8'	6.64 s	111.9	6.44 s	109.9
9'		133.2		125.8
10'		128.8		129.2
11'		172.0		172.6
12'	2.34 br d	42.3	2.35 br d	42.3
	2.21 br d		2.15 br d	
21-CN		118.0		118.7
N-CH ₃	2.21 s	41.6	2.19 s	41.6
6-CH ₃	2.03 s	9.7	2.04 s	9.7
16-CH ₃	2.33 s	15.8	2.32 s	15.8
17-OCH ₃	3.80 s	60.3	3.78 s	60.4
7'-OCH ₃	3.55 s	55.2	3.60 s	55.2
5-OCOCH ₃	2.27 s	20.4	2.26 s	20.4
5-OCOCH ₃		168.2		168.2
18-OH	5.76 br s		5.77 s	
6'-OH			5.59 s	

Several conditions have been successfully used to prepare the aromatic esters of Et 770 (**21-37**) such as using the corresponding acid chlorides, acid anhydrides or the acids with DCC as the coupling reagent. However, in case of the acid chloride or acid anhydride of indole-3-carboxylic acid failed to react with Et 770. On the other hand, Et 770 did react with indole-3-carboxylic acid in the presence of DCC to yield the acylated product **39** (65 % yield) occurring at N-2' instead of C-6' of the C'-subunit (Scheme 26)



Scheme 26. The reactions of Et 770 and indole-3-carboxylic acid bearing acid chloride, acid anhydride and the acid with DCC

HR-FABMS of 2'-*N*-3''-Indolecarboxylecteinasidin 770 (**39**) showed the $[M + H]^+$ ion peak at 914.3063 corresponding to the calculated $C_{49}H_{48}N_5O_{11}S$ (914.3071). This indicated that **39** was the mono acylated product. The indole carbonyl containing moiety showed the pattern of proton signals at δ 8.62 (1H, br s, NH), 8.06 (1H, d, $J = 7.9$ Hz, 4''-H), 7.68 (1H, d, $J = 2.7$ Hz, 2''-H), 7.64 (1H, d, $J = 7.9$ Hz, 7''-H), 7.38 (1H, ddd, $J = 7.9, 7.0, 0.9$ Hz, 5''-H or 6''-H), 7.27 (1H, ddd, $J = 7.9, 7.0, 1.2$ Hz, 5''-H or 6''-H), and carbon signals at δ 135.7 ppm (C-8''), 129.3 ppm (C-2''), 125.0 ppm (C-9''), 122.9 ppm (C-6'') and 122.6 ppm (C-4'').

In addition, no downfield shifted carbons of the aromatic parts in the *A*- and *C*-subunits were observed from the ^{13}C -NMR spectra as compared to those of **2** (Table 17). However, the downfield shifts were observed from the carbons adjacent to the nitrogen atom in the *C*-subunit, namely C-1' (δ 70.2 ppm), and C-12' (δ 46.6 ppm) in the ten membered sulfide bridge. The unusual upfield shifts of the *A*-subunit protons of **39** at δ 5.41 ppm (15-H), δ 3.37 ppm (17-OCH₃), and δ 1.14 ppm (16-CH₃) were also noted which could be explained by the shielding effects from the ring current of the indole ring attached at N-2' in the *C*-subunit. The characteristic of methylene protons at position-22 were somewhat upfield shifted to δ 4.62 (1H, d, $J = 11.3$ Hz), 4.54 (1H, dd, $J = 11.3, 1.8$ Hz) compared with **2** [δ 5.01 (d, $J = 11.6$ Hz), 4.12 (dd, $J = 11.6, 2.0$ Hz)].

The unsubstituted 18-OH and 6'-OH protons in the *A*- and *C*-subunits of **39** were also observed in the 1H -NMR spectrum at δ 5.61 ppm and δ 5.41 ppm, respectively as compared to those of **2** (δ 5.77 ppm and δ 5.59 ppm). Both OH signals were disappeared in the presence of deuterium dioxide (D₂O) (Figure 20).

D:\NMR DATA\plocnhip\indole-3-DCC770fr27-47-051101.als
indole-3-770-D2O-051121

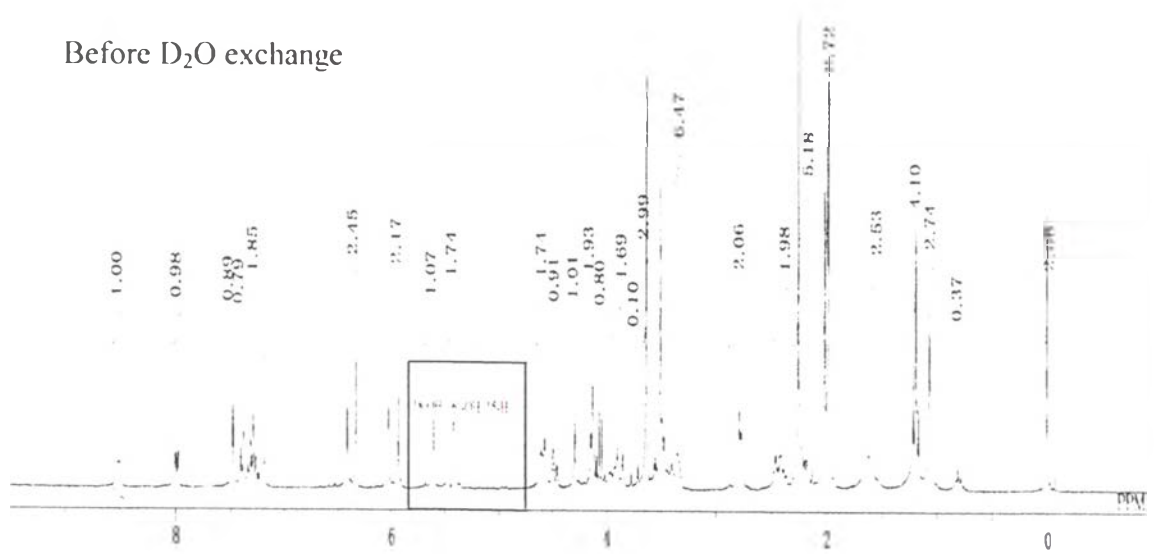
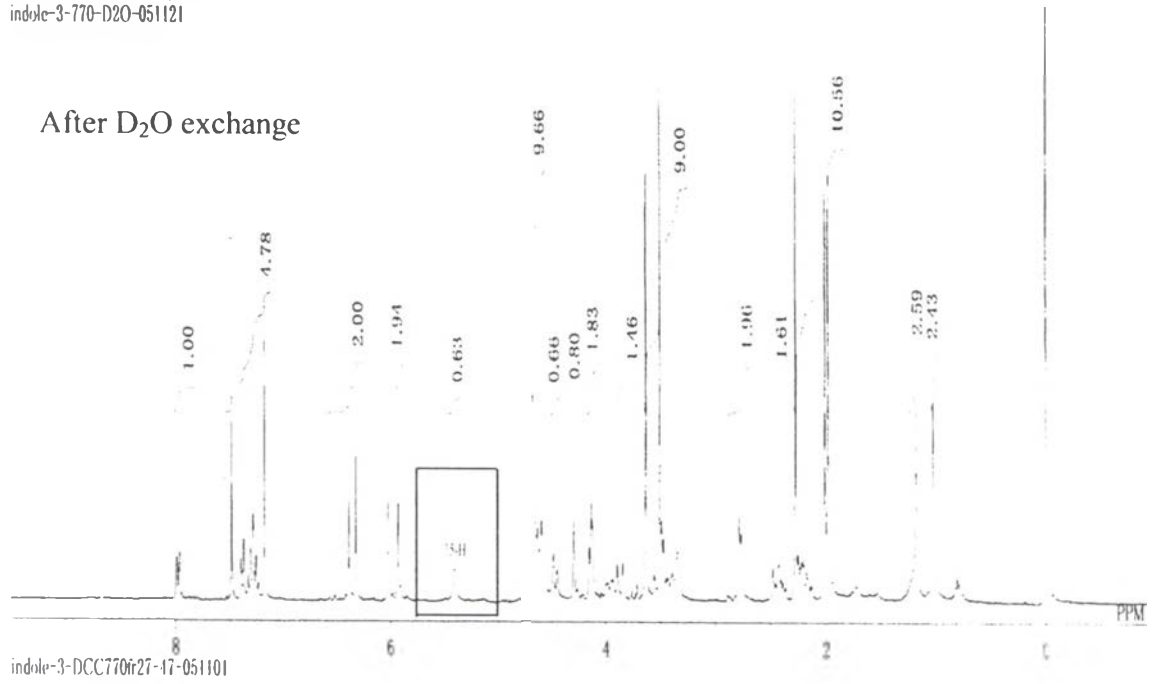


Figure 20. 300 MHz ¹H-NMR spectra of 2'-N-3''-Indolecarboxyl ecteinascidin 770 (**39**)

Table 17. Partial ^1H and ^{13}C -NMR spectra data of the core structures of Et 770 [2] and 2'-N-3"-Indolecarboxylecteinascidin 770 [39] recorded in CDCl_3

Positions	39		Et 770 [2]	
	$\delta_{\text{H}} J$ (Hz)	δ_{C}	$\delta_{\text{H}} J$ (Hz)	δ_{C}
1	4.36 s	60.7	4.32 s	61.2
3	3.50 d (4.9)	61.1	3.51 d (4.9)	59.7
4	4.62 br s	41.8	4.57	41.9
5		141.4		141.4
6		113.3		113.4
7		145.7		145.3
8		141.3		140.2
9		113.7		114.1
10		122.4		121.2
11	4.20 dd (5.0, 1.4)	54.9	4.28 dd (4.9, 1.2)	54.8
13	3.35 br t	54.9	3.41 br t	54.7
14	2.85 d (6.1)	24.9	2.91 d (7.6)	24.2
15	5.41 s	121.4	6.60 s	120.7
16		129.0		129.4
17		142.7		143.1
18		147.0		147.9
19		117.3		118.4
20		129.7		130.8
21	4.19 d (2.7)	59.8	4.18 d (2.8)	59.6
22	4.62 d (11.3)	60.3	5.01 d (11.6)	60.1
	4.54 dd (11.3, 1.8)		4.12 dd (11.6, 2.0)	
23	6.09 d (1.5)	101.9	6.04 d (1.2)	102.0
	5.99 d (1.5)		5.97 d (1.2)	
1'		70.2		64.9
3'	4.00 m	38.5	3.11 m	39.7
	2.49 m		2.79 m	
4'	2.49 m	29.7	2.60 m	28.8
	2.28 m		2.42 dt (15.9, 3.4)	
5'	6.40 s	113.7	6.46 s	114.2
6'		144.7		144.6
7'		144.6		144.7
8'	6.48 s	110.5	6.44 s	109.9
9'		127.5		125.8
10'		127.6		129.2
11'		170.6		172.6
12'	3.94 d (11.3)	46.6	2.35 br d	42.3
	3.47 br d		2.15 br d	
21-CN		118.3		118.7
N-CH ₃	2.09 s	41.6	2.19 s	41.6
6-CH ₃	2.05 s	9.8	2.04 s	9.7
16-CH ₃	1.14 s	14.2	2.32 s	15.8
17-OCH ₃	3.57 s	59.8	3.78 s	60.4
7'-OCH ₃	3.71 s	55.3	3.60 s	55.2
5-OCOCH ₃	2.30 s	20.4	2.26 s	20.4
5-O $\underline{\text{C}}$ COCH ₃		168.2		168.2
18-OH	5.61 br s		5.77 s	
6'-OH	5.41 s		5.59 s	

3. Cytotoxic activity of the ecteinascidin analogs

The biological activities of the synthesized ester derivatives of Ets 770, 786 and 743 were studied on the antiproliferative assay, using three human cancer cell lines, including colon carcinoma (HCT116), lung carcinoma (QG56) and prostate cancer (DU145). The biological data obtained are shown in Table 18 and Figure 21 represented the structural modification of ecteinascidin molecule. The ecteinascidin 770 18,6'-diacetyl (**18**) and ecteinascidin 743 18,6'-diacetyl (**20**) exhibited significantly comparable activities in the tested model, but were 4-7 folds less active for QG56 and DU145, and 32-35 folds less active for HCT116 than those of their natural parent compound (Et 770). The reduction in potency of those esterified analogs may result from the lack of hydrogen donor bonding in the *A*-subunit which ultimately decreased the stability of DNA-adduct. Unfortunately, the diacetate **19**, derived from Et 786 exhibited up to 100 folds less active on three human cancer cell lines than **18**, **20** and their parent Et 770. The similar profile on cytotoxic activities of **18** and **20** suggested the possibility of **18** to eliminate cyano moiety and resulted the active alkylating iminium species within the testing cell cultures.

The antiproliferative activities of those obtained aromatic acid esters were also studied on HCT116, QG56 and DU145 cell lines and the results are shown in Table 18. The cytotoxic activity of the series of the nitro (**22-24**) and the methoxy (**28-29**) substitutions on the phenyl ring provided enhancing effect on the potency whereas the bromo substitution (**25-27**) diminishing the potency when compared to their benzoyl analog (**21**). Pattern of substitution also affected the observed potency, the higher potency was observed in the *p*-substitution of nitro (**22**) and methoxy (**28**) substitution series. However, the data was not sufficient to conclude and relationship between activity and electron-donating or electron-withdrawing substitutions on the phenyl ring. On the other hand, the naphthoyl derivatives (**32-33**) representing bulky group resulted in dramatically diminished cytotoxicity when compared to the benzoyl and their substitution series analogs.

Moreover, the other *N*-containing heterocyclic derivatives such as, pyridinoyl, quinolinoyl and isoquinolinoyl were prepared and also evaluated for their activities. The cytotoxicity data revealed that those analogs showed closely correlation with the corresponding *p*-substitution on the phenyl ring (**22** and **28**). The 2-quinolinoyl (**34**) analog was somewhat more potent than **21**, while 4-quinolinoyl (**35**) and isoquinolinoyls (**36-37**) were less active than **21** and pyridinoyls (**30-31**). It is noteworthy that the substitution on phenolic hydroxyl at the *C*-subunit bearing *p*-substitution on phenyl ring (**22** and **28**) and pyridinoyl substituent (**30-31**) possessed higher cytotoxicity than the other analogs.

Surprisingly, 2'-*N*'-3"-indolecarboxylecteinascidin 770 (**39**), which was acylated at *N*-2' of the *C*-subunit exhibited high activity. As shown in Table 18, **39** exhibited activity superior to the parent **2** against HCT116, QG56 and DU145. It was also noteworthy that **39** showed the highest cytotoxicity and exhibited selectivity for human colon carcinoma cell line; HCT116.

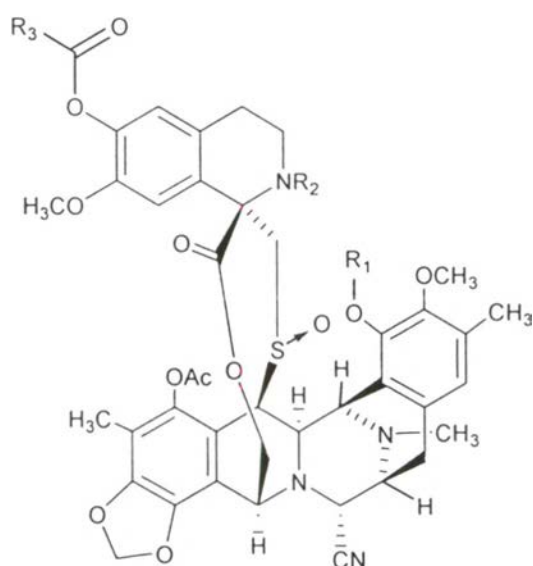
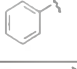
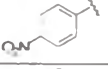
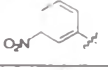
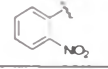
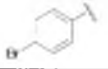
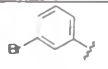
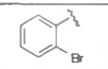
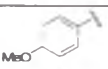
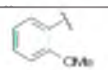
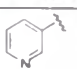

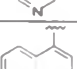
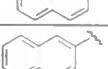
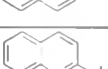

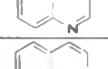
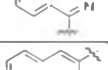
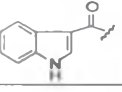


Figure 21. Structure of the acylated of eccinascidins

Table 18. Cytotoxicity of ecteinascidin 770 acylated compounds to various cancer cell lines (IC_{50} nM)^a

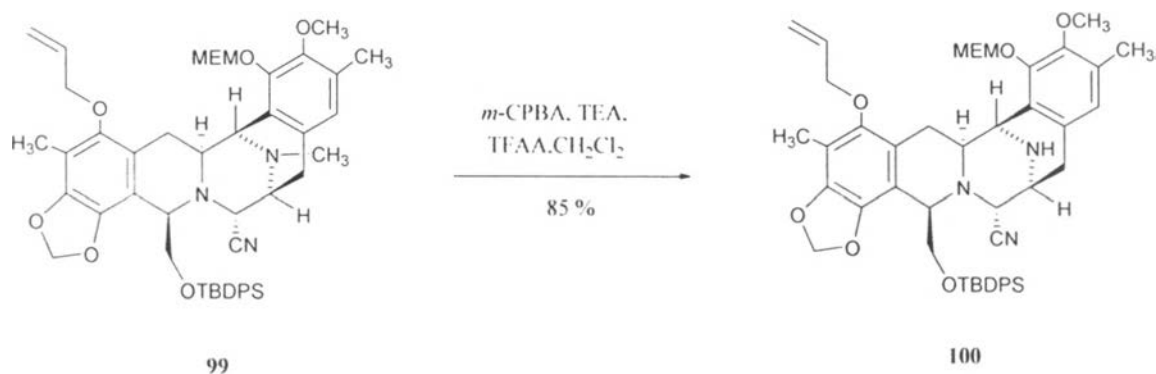
Cpds	R ₁	R ₂	R ₃	IC ₅₀ (nM)		
				HCT116	QG56	DU145
Et 770	H	H	H	0.04	1.8	0.66
18 (Et 770)	Ac	H	CH ₃	1.4	8.3	4.4
19 (Et 786)	Ac	H	CH ₃	160	220	200
20 (Et 743)	Ac	H	CH ₃	1.3	9.5	4.4
21	H	H		0.68	3.2	1.1
22	H	H		0.26	0.96	0.37
23	H	H		0.49	3.3	1.6
24	H	H		1.9	7.1	2.7
25	H	H		15	36	16
26	H	H		7.1	39	11
27	H	H		4.2	19	7.6
28	H	H		0.31	1.7	0.62
29	H	H		0.62	3.6	1.1
30	H	H		0.20	1.0	0.51
31	H	H		0.15	0.87	0.48
32	H	H		13	36	24
33	H	H		6.3	24	12
34	H	H		0.41	2.4	0.95
35	H	H		2.1	9.5	4.5
36	H	H		0.64	1.9	0.83
37	H	H		0.62	2.1	1.5
39	H		H	0.07	0.53	0.37

^aHCT116 = human colon carcinoma; QG56 = human lung carcinoma; DU145 = human prostate carcinoma.

4. Selective *N*-demethylation on ABC ring system with CAN

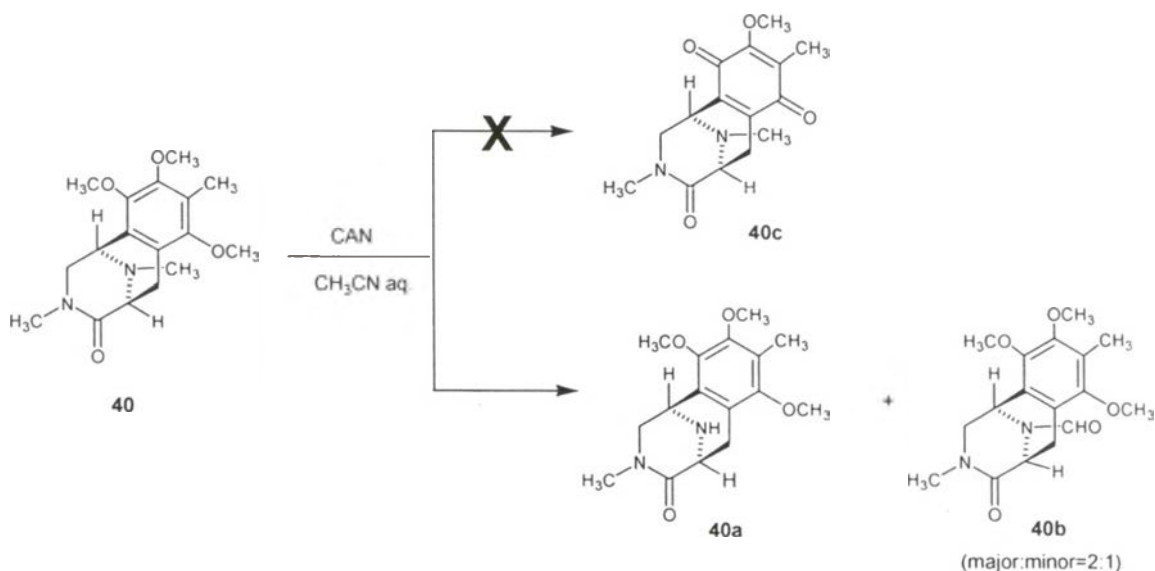
Several related model compounds of ecteinascidin molecule will be employed for this study. As part of our studies to find the optimized method for *N*-demethylation of ecteinascidin alkaloid. The simplified structures of safracin bearing ABC ring model, which contained *N*-methyl, were previously synthesized by Kubo group (Saito, *et al.* 1992; 2000; 2003). All of the synthetic model compounds represent the *A*-subunit of ecteinascidin molecule, but bearing some viable substitution pattern on the ring as shown in Figure 3.

The different conditions for *N*-demethylation of tertiary amine such as ruthenium-catalyzed reaction (Murahashi *et al.*, 1988; 1992), methyl chloroformate and hydrazine (Csutoras *et al.*, 2004) were described. However, the application of all described reactions with **99** were failed to *N*-demethylation. In contrast, the Polonovsky reaction [*m*-CPBA in the presence of TEA, TFAA, and CH_2Cl_2] (Frohlic *et al.*, 1998) could be used to demethylate, resulting **100** in high yield (Scheme 27) (Menchaca *et al.*, 2003).



Scheme 27. The Polonovsky reaction of **99**

The oxidative demethylation of cerium (IV) ammonium nitrate (CAN) is an alternative method to prepare quinone functionality (Spyroudis, 2000). However, Saito's group failed to prepare quinone **40c** from **40** under the condition of CAN (2.4 equimolar), but the reaction led to undesired products as *N*-demethyl compound **40a** in 73% yield (Scheme 28 and Table 19). Therefore, oxidative *N*-demethylation of the model compounds were carried out in various amounts of CAN in this study. The optimal amount of CAN is 5 equimolars resulted that 1,2,3,4,5,6-hexahydro-7,9,10-trimethoxy-3,8-dimethyl-4-oxo-1,5-imino-3-benzazocin **40a** in the range of 73-89 % yield and 1,2,3,4,5,6-hexahydro-7,9,10-trimethoxy-3,8-dimethyl-4-oxo-1,5-imino-11-carbonyl-3-benzazocin **40b** (3-8 % yield) as the side products (Table 19). Slowly addition of CAN solution in several portions into the reaction mixture led to 89 % yield. The different conditions by changing solvent to THF or 1,4-dioxane instead CH₃CN gave diminishing yield of the products. The other model compounds **41**, **42**, **46**, and **47** could also be succeeded *N*-demethylation with CAN as shown in Schemes 29 and 30, and Table 20. The quinone moiety obtained in **43** was also prepared by *N*-demethylation under CAN condition (Scheme 31)



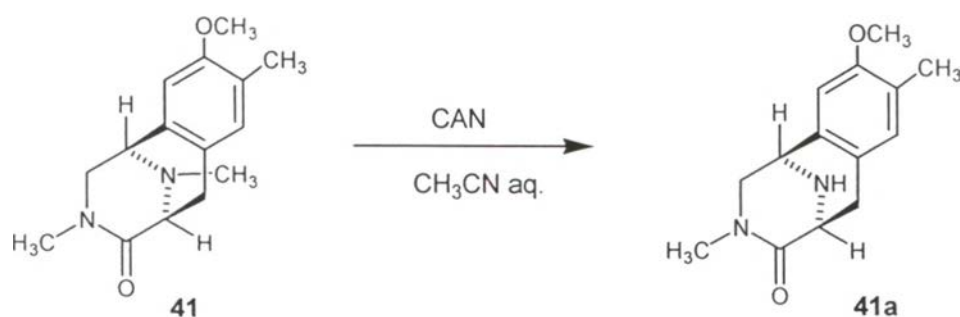
Scheme 28. The oxidative *N*-demethylation of **40** with CAN

Table 19. The different conditions of oxidative *N*-demethylation of **40** with CAN

Reaction scale	Solvent	CAN	40a	40b	40 (recover)
32.8 mg (0.103 mM)	CH ₃ CN	2.4 eq	73 %	-	-
32.0 mg (0.1 mM)	CH ₃ CN	5.0 eq	81 %	8 %	-
32.0 mg (0.1 mM)	CH ₃ CN	5.0 eq ^a	73 %	-	-
32.0 mg (0.1 mM)	CH ₃ CN	5.0 eq ^b	89 %	3 %	5 %
32.0 mg (0.1 mM)	THF	5.0 eq ^b	62 %	1 %	5 %
32.0 mg (0.1 mM)	1,4-dioxane	5.0 eq	76 %	1 %	-

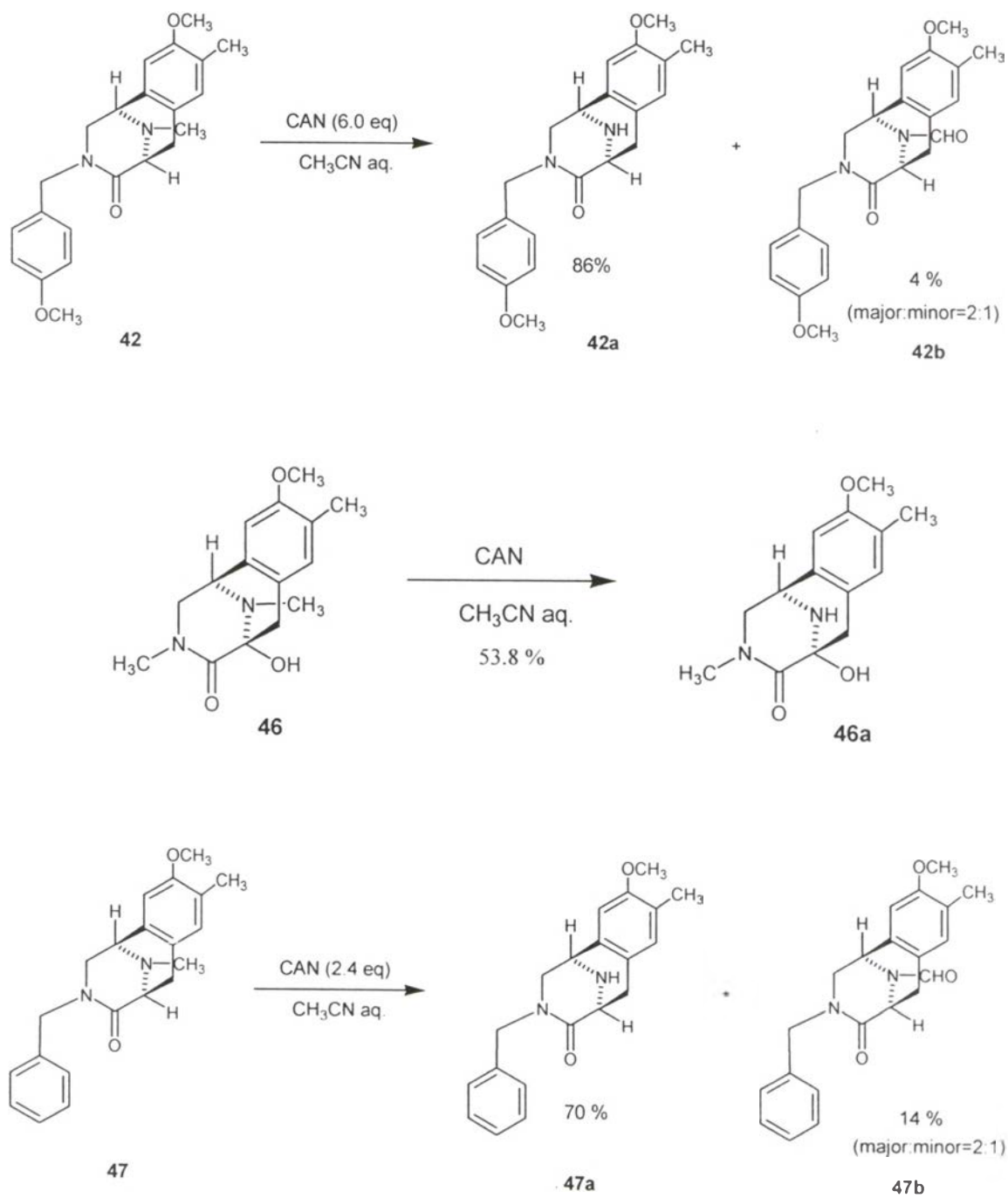
a) added CAN in two times (1.2 eq. + 3.8 eq.)

b) added CAN in four times (2.4 eq. + 0.6 eq. + 1.0 eq. + 1.0 eq.)

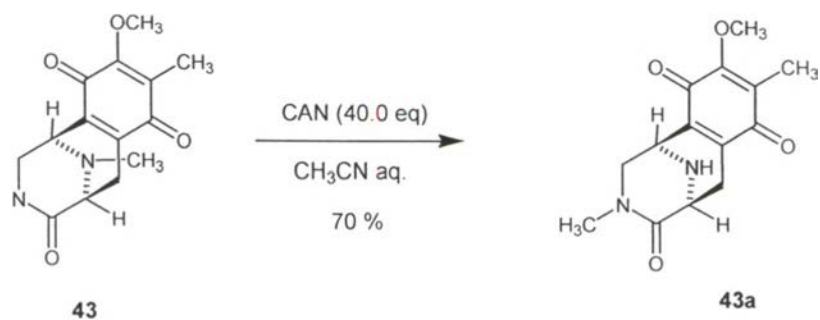
Scheme 29. The oxidative *N*-demethylation of **41** with CANTable 20. The different condition of oxidative *N*-demethylation of **41** with CAN

reaction amount	Solvent	CAN	41a	41 (recover)
26.0 mg (0.1 mM)	CH ₃ CN	2.4 eq	73 %	-
26.0 mg (0.1 mM)	CH ₃ CN	5.0 ^a eq	78 %	-
26.0 mg (0.1 mM)	CH ₃ CN	5.0 ^a eq	90 %	6 %

a) added CAN in three times (1.5 eq. + 1.5 eq. + 2.0 eq.)



Scheme 30. The oxidative *N*-demethylation of **42**, **46** and **47** with CAN



Scheme 31. The oxidative *N*-demethylation of **43** containing the quinone moiety with CAN

The prepared *N*-demethyl and *N*-formyl compounds were elucidated predominantly by interpretation of ¹H-NMR. The absence signal of *N*-methyl proton at δ 2.42 ppm and also the increasing polarity of the product, which was appeared the lower R_f value on TLC in the mixture solution of chloroform-methanol (10:1) as eluting solvent, confirmed the *N*-demethylation product. The *N*-formyl product was also confirmed by the disappearance of the *N*-methyl proton signal, whereas the formyl proton signal exhibited two rotamers with the chemical shifts in the range δ 8.1-8.3 ppm (Figure 22)

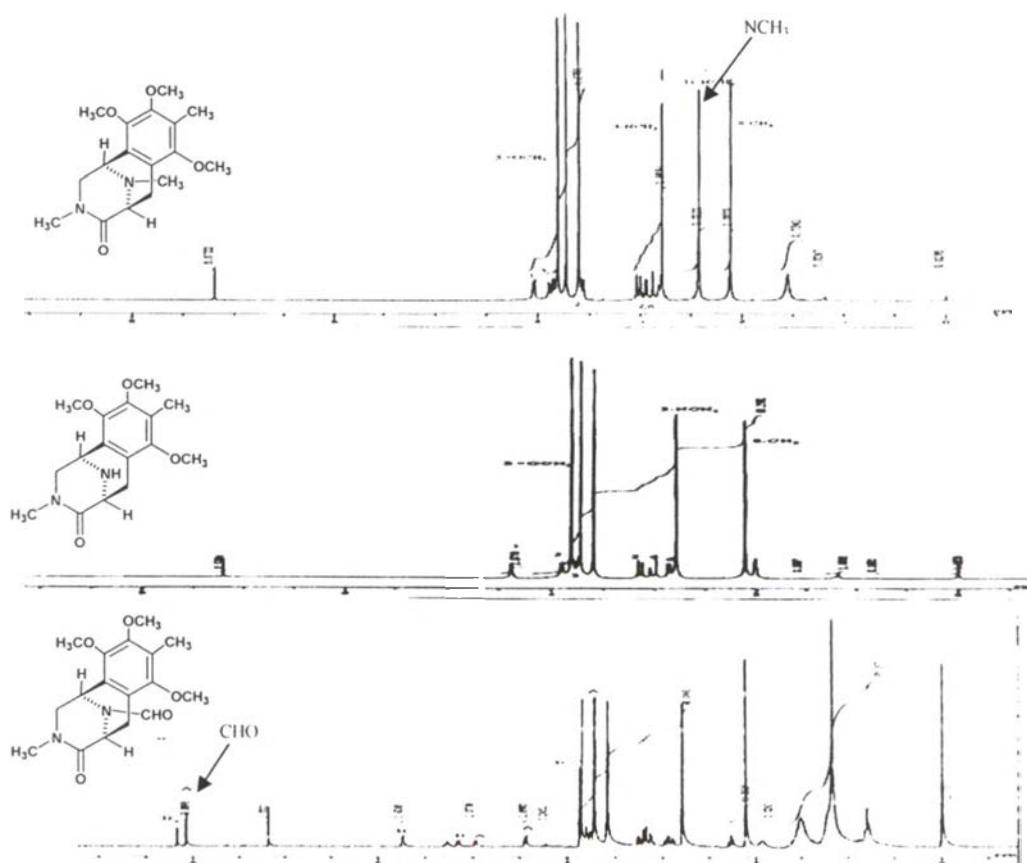
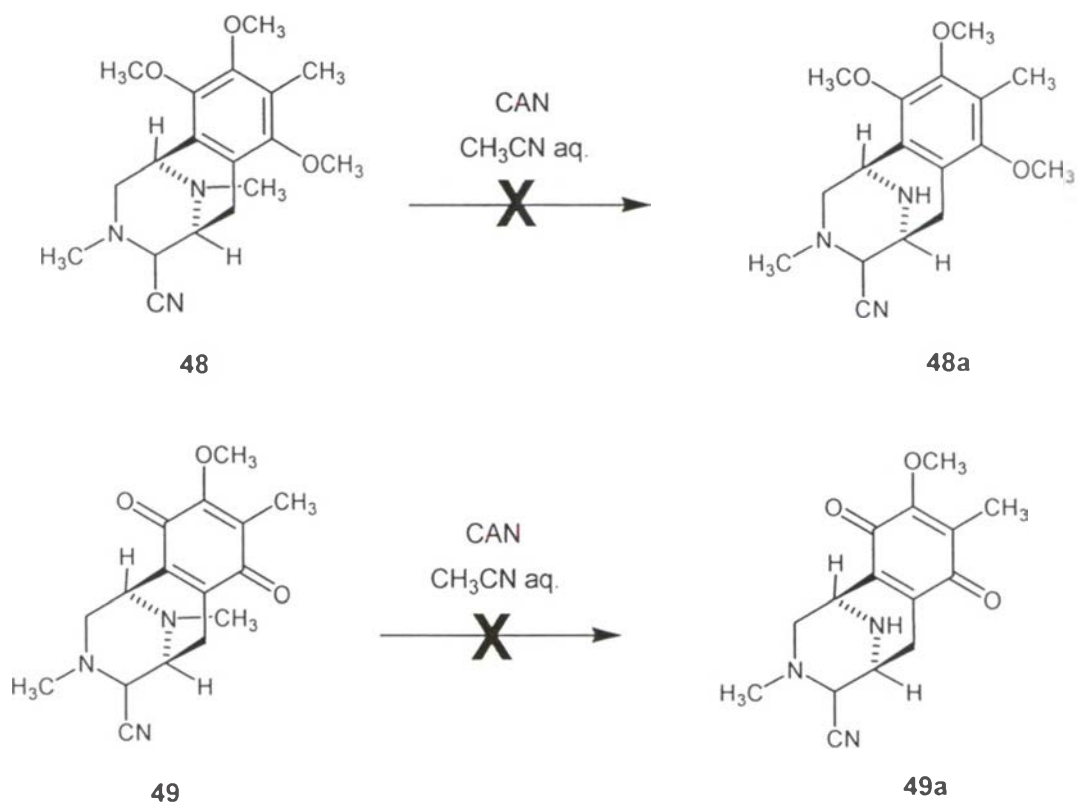


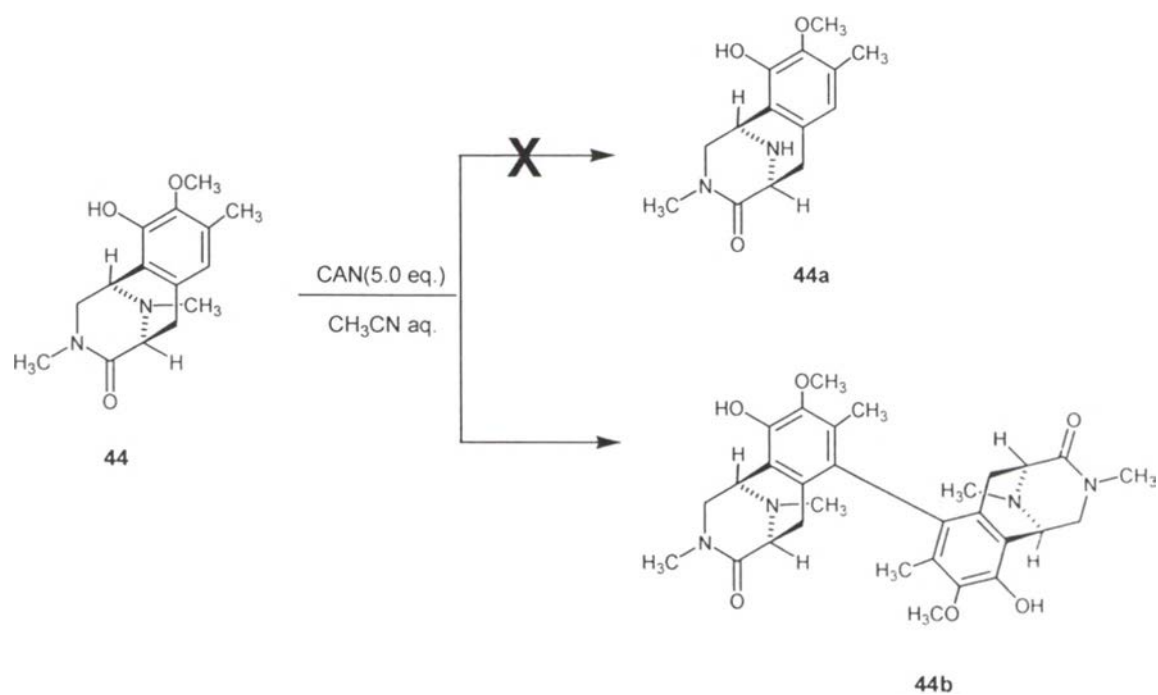
Figure 22. ¹H-NMR spectra of **40**, **40a**, and **40b**

In the case of compounds **48** and **49** which bearing the cyanoamine functionality, no reaction was observed under the condition of CAN 5 equimolars (Scheme 32), and decomposition was observed under 40 equimolars of CAN.



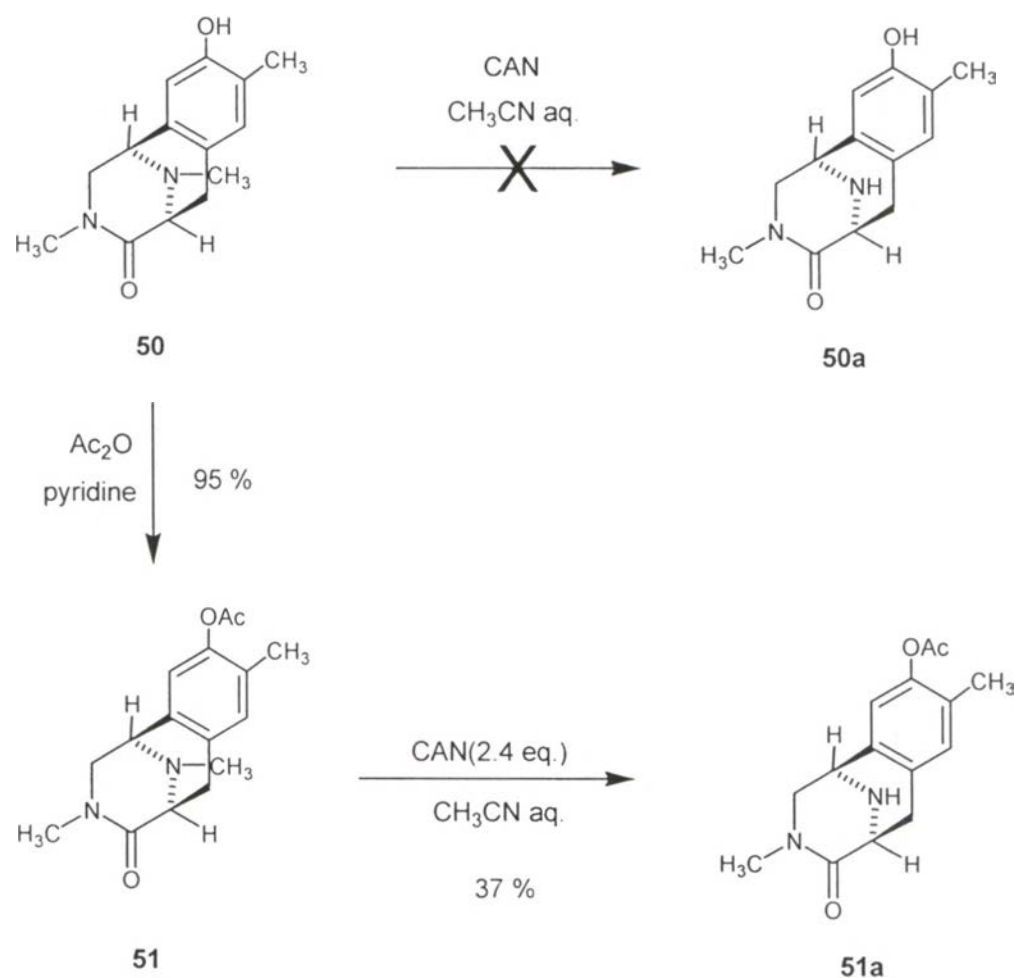
Scheme 32. The oxidative N-demethylation of **48** and **49** containing cyanoamine group with CAN

The model compound **44**, which bearing the substitution pattern on the aromatic ring related to the *A*-subunit of ecteinascidin, while the cyanoamine moiety was replaced with the amide group was also studied. Under the condition of CAN 5 equivalents and **44**, the undesired dimeric product **44b** (1,2,3,4,5,6-hexahydro-7,9,10-trimethoxy-3,8-dimethyl-4-oxo-1,5-imino-11-carbonyl-3-benzazocin) was obtained instead of the *N*-demethyl product (Scheme 33). Mass spectral data showed the $[M]^+$ ion at m/z 550 corresponding to $C_{30}H_{38}O_6N_4$ (calcd for 550.2791). In the 1H -NMR spectrum, the disappearance of the signal of 7-H (δ 6.85 ppm) at the aromatic ring confirmed that the dimer compound **44b** was obtained. CAN might generate radical of **44** to form the dimer compound **44b**.



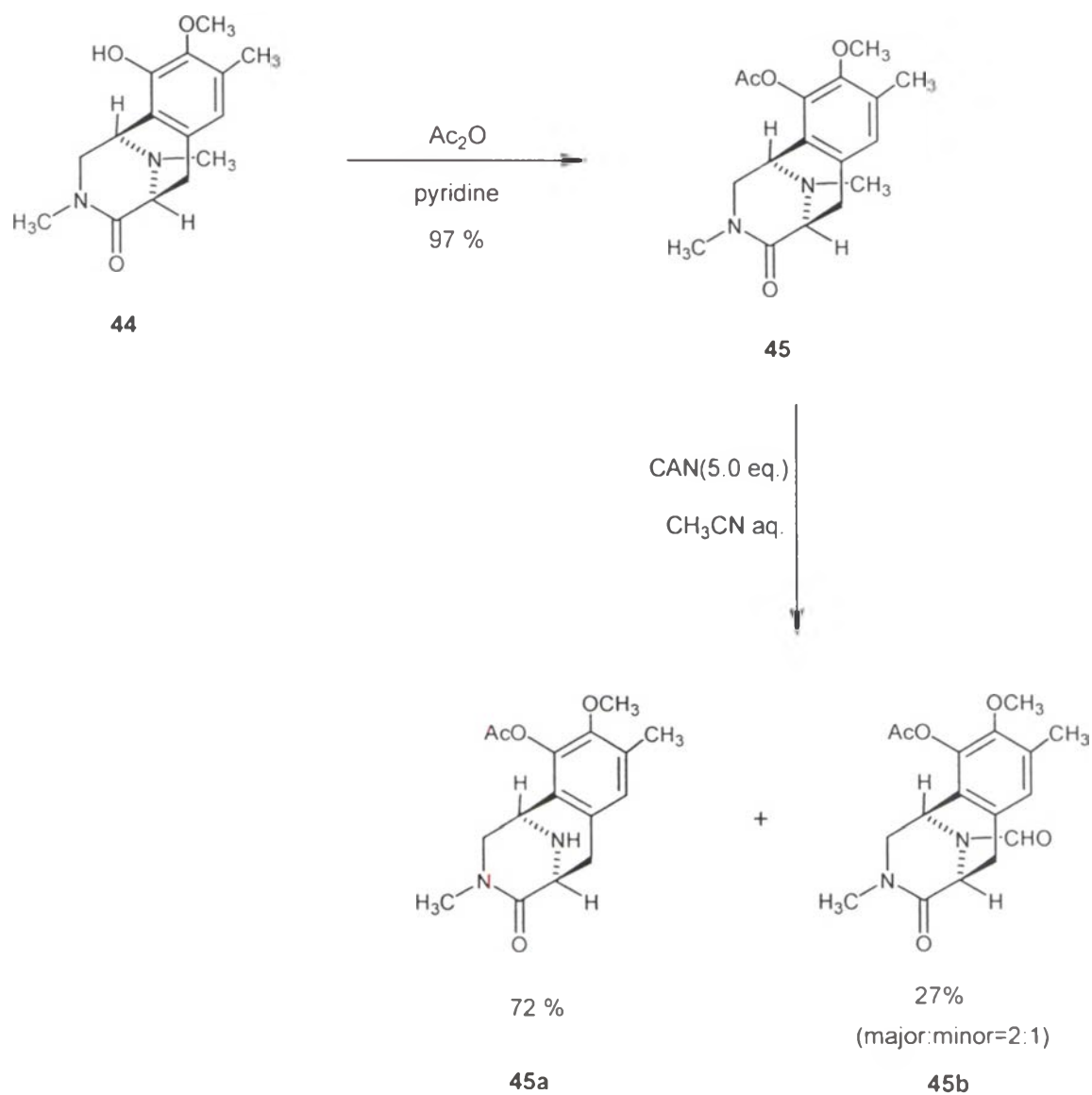
Scheme 33. The oxidative *N*-demethylation of **44** with CAN

According to Saito's group report (unpublish data). CAN failed to demethylate **50** and led to unaltered starting material. However, upon acetylation of **50** to protect the hydroxyl functionality obtained **51**. Subsequently, the *N*-demethylation of **51** with CAN was achieved with **51** to give *N*-demethyl product **51a** in 37 % yield (Scheme 34).



Scheme 34. The acetylation reaction and the oxidative *N*-demethylation of **50** with CAN

Therefore, **44** was protected with an acetyl group as described for **50**, to yield **45** in 95 %. The reaction with CAN was further reacted with **45** to afford the corresponding *N*-demethylation compound **45a** (72 % yield) and *N*-formyl compound **45b** (27 % yield) as shown in Scheme 35. For the successful of *N*-demethylation of the model compound **44** is worthy to work in advance with the natural ecteinascidin.



Scheme 35. The acetylation reaction and the oxidative *N*-demethylation of **44** with CAN